

## Article

# Depth–Sequential Investigation of Major Ions, $\delta^{18}\text{O}$ , $\delta^2\text{H}$ and $\delta^{13}\text{C}$ in Fractured Aquifers of the St. Lawrence Lowlands (Quebec, Canada) Using Passive Samplers

Guillaume Meyzonnat <sup>1,\*</sup>, Florent Barbecot <sup>1</sup>, José Corcho Alvarado <sup>2</sup>, Daniele Luigi Pinti <sup>1</sup>,  
Jean-Marc Lauzon <sup>3</sup> and Renald McCormack <sup>4</sup>

<sup>1</sup> Centre Geotop, Department of Earth and Atmospheric Sciences, Faculty of Sciences, University of Quebec in Montreal, Montreal, QC H3C 3P8, Canada; barbecot.florent@uqam.ca (F.B.); pinti.daniele@uqam.ca (D.L.P.)

<sup>2</sup> Spiez Laboratory, Federal Office for Civil Protection, 3700 Spiez, Switzerland; Jose.Corcho@babs.admin.ch

<sup>3</sup> TechnoRem Inc., Laval, QC H7P 6G5, Canada; jean-marc.lauzon@technorem.com

<sup>4</sup> Envir'Eau-Puits Inc., Lévis, QC G7A 3V3, Canada; rmccormack@envireaupuits.com

\* Correspondence: meyzonnat.guillaume@uqam.ca

**Abstract:** General and isotopic geochemistry of groundwater is an essential tool to decipher hydrogeological contexts and flow paths. Different hydrogeochemical patterns may result from the inherent physical aquifer heterogeneity, which may go unnoticed without detailed investigations gathered from multilevel or multiple observation wells. An alternative to overcome the frequent unavailability of multiple wellbores at sites is to perform a detailed investigation on the single wellbore available. In this perspective, the aim of this study is to use passive samplers to sequentially collect groundwater at depths in long–screened wellbores. Such investigation is carried out for major ions and stable isotopes compositions ( $\delta^2\text{H}$ ,  $\delta^{18}\text{O}$ ,  $\delta^{13}\text{C}$ ) at ten sites in the context of fractured carbonate aquifers of the St. Lawrence Lowlands (Quebec, Canada). The information gathered from the calco–carbonic system, major ions and stable isotopes report poorly stratified and evolved groundwater bodies. Contribution of water impacted by anthropogenic activities, such as road salts pollution and carbon sources from C4 vegetation, when they occur, are even observed at the greatest depths. Such observations suggest quick flow paths and efficient mixing conditions, which leads to significant contributions of contemporary groundwater bodies in the fractured aquifers investigated down to depths of about 100 m. Although physical aquifer investigation reported few and heterogeneously distributed fractures per wellbore, hydrogeochemical findings point to at overall well interconnected fracture networks in the aquifer and high vulnerability of groundwater, even at significant depths.

**Keywords:** passive water sampling; long screened wellbore; fractured aquifer; major ions chemistry; stable isotopes of water and of carbon; St. Lawrence lowlands



**Citation:** Meyzonnat, G.; Barbecot, F.; Corcho Alvarado, J.; Pinti, D.L.; Lauzon, J.-M.; McCormack, R. Depth–Sequential Investigation of Major Ions,  $\delta^{18}\text{O}$ ,  $\delta^2\text{H}$  and  $\delta^{13}\text{C}$  in Fractured Aquifers of the St. Lawrence Lowlands (Quebec, Canada) Using Passive Samplers. *Water* **2021**, *13*, 1806. <https://doi.org/10.3390/w13131806>

Academic Editor: Aldo Fiori

Received: 1 June 2021

Accepted: 28 June 2021

Published: 29 June 2021

**Publisher's Note:** MDPI stays neutral with regard to jurisdictional claims in published maps and institutional affiliations.



**Copyright:** © 2021 by the authors. Licensee MDPI, Basel, Switzerland. This article is an open access article distributed under the terms and conditions of the Creative Commons Attribution (CC BY) license (<https://creativecommons.org/licenses/by/4.0/>).

## 1. Introduction

The chemical and isotopic study of groundwater, usually termed “hydrogeochemistry” is an essential complement to physical studies to identify recharge and discharge zones, flow paths and water chemical evolution [1]. As it reflects inputs from recharge areas [2], as well as confinement conditions [3], hydrogeochemistry is also used in certain cases as a proxy for groundwater vulnerability [4]. Yet, hydrogeochemistry studies suffer the same limitations as those in physical hydrology: flow path reconstructions or chemical evolution of water are often based on limited spatial access to the aquifer, through the measurements, when available, in piezometers, water wells and natural sources. Measured physical and chemical parameters of groundwater from these sparse and limited locations are often assumed to represent the whole aquifer situation.

Recently, numerous hydrogeological regional studies were held in Quebec [5], and most of them have focused on groundwater geochemistry [1,6–16]. These studies have

considerably increased the amount of geochemical and isotopic data available for linking water composition and quality with confinement conditions at regional scale. However, as in most hydrogeochemical studies, conventional sampling was usually performed by collecting groundwater at the well discharge. Such sampling represents the mixture of water from all the productive intervals that may be present within a well, not allowing to discern if any chemical stratification is present. The reality is that aquifers are in most of the cases physically heterogeneous and may consequently contain chemically stratified groundwater, which may go unnoticed in the case of the conventional sampling. Chemical stratification is theoretically anticipated according to hydraulic ages for homogeneous aquifers [17] and have been reported in real cases for homogeneous sandy aquifers [18,19]. Hydrogeochemical stratification is also reported in heterogeneous contexts with successive aquifer/aquitard arrangements [20,21].

As multilevel or successive observation wells are not often available, one opportunity to investigate the occurrence of hydrogeochemical stratification is to perform a depth-sequential sampling in a single long screened wellbore [22]. However, such sampling remains uncommon [23] as it increases operating costs, handling and technicality, especially for significant depths. Uncertainties may also arise regarding the representativeness of the water sample with respect to depth. For instance, isolating a section of a wellbore with packers does not preclude bypass flows from the outside due to interconnected fractures [24]. Other low flow pumping methods at depth may also be difficult to handle due to equipment clutter and blockage (submersible pumps, tubing and cables), because sections in wellbores are usually narrow. One simpler alternative to sample sequentially in long screened wellbores is to use passive samplers. Passive sampling refers to the collection of water through physically driven solute transport. This naturally induced transport leads to the equilibration of the water within the sampler with the groundwater composition, without usage of any mechanical or electrical device.

This research aims to investigate about the presence of groundwater chemically stratified with the depth in fractured aquifers. According to the references cited above, this information is not well known in the study area, and is also generally not investigated during hydrogeological studies, as one single composite groundwater samples is usually gathered for each site at the pumping's discharge. Innovative aspects of this research thus relate to the acquisition of a new type of hydrogeochemical dataset in the region, and to the development of a new sampling method using passive samplers. The relevance of such sampling is demonstrated with major ions and stable isotopes ( $\delta^2\text{H}$ ,  $\delta^{18}\text{O}$ ,  $\delta^{13}\text{C}$ ). The passive sampling is organized upon data previously gathered from physical borehole logging and is operated sequentially at depths up to 100 m in the St. Lawrence Lowlands, Quebec, Canada. The investigation was implemented in long screened wellbores (e.g., exceeding 50 m depth) in fractured aquifers to report, if occurring, the largest possible ranges of groundwater geochemical compositions with the depth. Granular aquifers were not considered during this study, as borehole screens in the area are often installed at shallow depths, and always over relatively short intervals (i.e., usually less than 5 m long), providing less favorable conditions to highlight the occurrence of hydrogeochemical stratification, if any.

## 2. Geological and Hydrogeochemical Settings

### 2.1. Geology of the Studied Area and Lithology of the Sampled Wellbores

This study targeted water wells located in the St. Lawrence Lowlands, which is an extended relatively flat area between Montreal and Quebec (Figure 1). Targeted aquifers are sedimentary and metasedimentary formations belonging to two distinct geological provinces: the St. Lawrence Platform in the northwestern portion of the area and the Appalachian Mountains in the southeastern portion of the area. The St. Lawrence Platform is a Cambrian–Lower Ordovician siliciclastic and carbonate platform [25], formed in an extensional context related to the opening of the Iapetus Ocean and overlain by Middle–Late Ordovician foreland carbonate–clastic deposits, deposited during the closure of Iapetus

and the Appalachian Mountains buildup. The Appalachian Mountains is a two-stage orogen built up starting from the Ordovician (Taconic orogen [26]). Sedimentary units are represented in Figure 1 as a simplified version of the detailed mapping by [27]. The geomorphology of Quebec is marked by glaciation–deglaciation phases, which controlled the deposition of unconsolidated sediments overlying the bedrock [28,29]. The nature of these unconsolidated sediments largely controls the recharge and confinement conditions of the fractured aquifers [30].

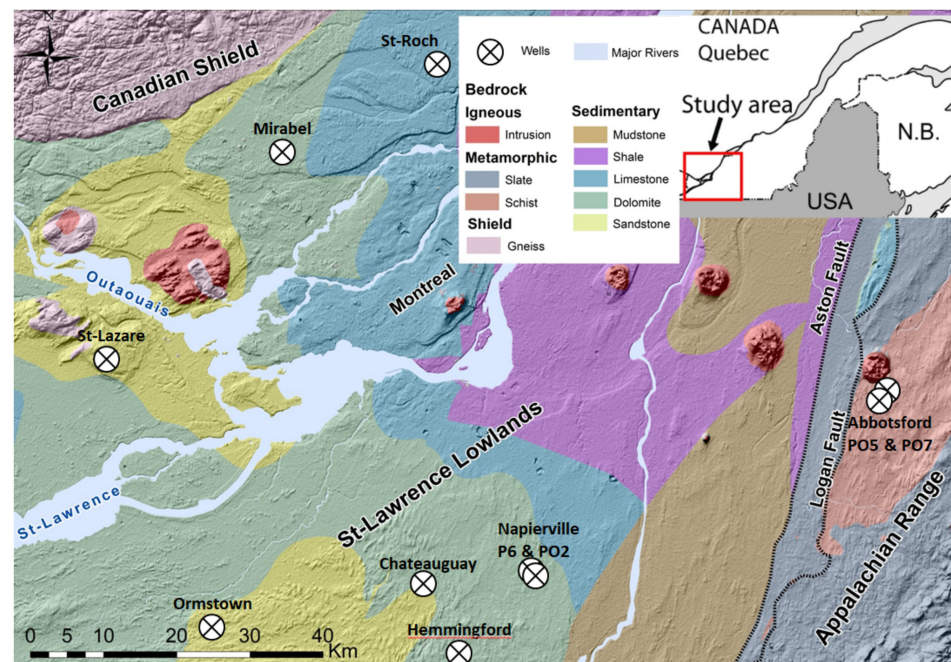


**Figure 1.** Geological map of the investigated area, with localization of the wellbores.

Ten municipal and observation wells were studied and named depending on their locations. St. Lazare and Ormstown wellbores were drilled and installed in Cambrian sandstone of the Potsdam Group; Mirabel, Napierville and Hemmingford wellbores in Ordovician dolomite of the Beekmantown Group; St. Roch wellbore in the Ordovician limestone of the Trenton Group and the Chateauguay wellbore is located in the transition zone between the Postdam and the Beekmantown Groups. To the west, Abbotsford wellbores are installed in the Mawcook Formation, composed of red schists. Confinement conditions at the location of the wellbores are inferred from the nature and the thickness of the sedimentary cover: unconfined condition for Abbotsford PO5 and Abbotsford PO7 (5 and 8 m of sand with silt lenses), Hemmingford (0.6 m of till), Ormstown (2.1 m of till), Napierville P6 (5 m of sand and gravel and 2 m of till), St. Roch (7.7 m of sandy till); semi-confined conditions for Mirabel (7.7 m of sandy deposits alternated with till); confined condition for St. Lazare (total of 62 m of sediments, mainly sands with silt lenses interlayered at the centre by a 6 to 10 m thick clayey till), Napierville PO2 (total of 15.6 m of sediments, alternating with sands, till and with a silt layer of 6 m thick), Chateauguay (13.4 m of clay, 1 m of till). All investigated wellbores have a diameter of 150 mm, are steel cased within unconsolidated sediments, and the casing is anchored into the bedrock (generally more than 1 m into it). Boreholes are uncased below the steel tubing. Characteristics of the wellbores are depicted in the synthetic logging including steel casing lengths, total borehole depths and depths to the water table (Section 3.3).

## 2.2. Hydrogeochemical Processes of Interest within the Studied Area

For fractured carbonate aquifers located within St. Lawrence Lowlands, dominant hydrogeochemical processes are carbonate weathering, dissolution/input of highly soluble

minerals (e.g., gypsum), calcium–sodium (Ca–Na) cationic exchanges and sodium chloride (Na–Cl) inputs from the Champlain Sea marine invasion [6,7,11,12,14,15].

Carbonate weathering results from the neutralization of carbonic acid inherited at recharge from the solubilization of CO<sub>2</sub> and leads to the production of bicarbonate as well as calcium (Ca<sup>2+</sup>) and magnesium (Mg<sup>2+</sup>) in groundwater [20]. The weathering capacity depends on the amount of CO<sub>2</sub> that can be dissolved in the water during the recharge. This amount is determined by the partial pressure of CO<sub>2</sub> in soils, as well as conditions that enhance the dissolution of CO<sub>2</sub> in water within the unsaturated zone such as the residence time and the nature of the porous matrix that favours the interaction between CO<sub>2</sub> and water [31]. Highest pCO<sub>2</sub> at the recharge are derived from the decomposition of organic matter in soils (ranging from 10<sup>−2.5</sup> to 10<sup>−1.5</sup> atm.), while atmospheric pCO<sub>2</sub> are much lower (10<sup>−3.4</sup> atm.) [31,32]. Partial CO<sub>2</sub> pressure in groundwater (pCO<sub>2</sub>) can be calculated from alkalinity and pH and allows distinguishing about the system openness to soil CO<sub>2</sub>. Although “fully open or closed systems” terminology is conceptually necessary to describe the calco–carbonic evolution of groundwater, “system openness to soil CO<sub>2</sub>” terminology is preferred as natural systems are in most of the case “partially open or closed” [31,33]. In the context of this study, carbonates in the St. Lawrence Lowlands include calcareous and dolomitic materials in variable proportion [27], such as for the Beekmantown and Trenton Group, and Appalachian’s Mawcook Fm. Quaternary unconsolidated sediments, notably tills, would also be a major source of carbonates [34].

Other insights about carbonate chemistry may be given by the calco–carbonic system as well as the isotopic composition ( $\delta^{13}\text{C}_{\text{DIC}}$ ) of the dissolved inorganic carbon (DIC) [35]. In a system theoretically fully open to CO<sub>2</sub>,  $\delta^{13}\text{C}_{\text{DIC}}$  will be enriched of about 10‰ (at 8.5 °C, range of temperature of the groundwater in this study) with respect to soil CO<sub>2</sub>  $\delta^{13}\text{C}_{\text{g}}$  because of isotopic fractionation between the DIC and the soil CO<sub>2</sub> that are in continual exchange. During calcite dissolution,  $\delta^{13}\text{C}_{\text{DIC}}$  evolves from the depleted isotopic composition of soil CO<sub>2</sub> ( $\delta^{13}\text{C}_{\text{g}}$ ) towards the more enriched composition of the carbonates ( $\delta^{13}\text{C}_{\text{s}}$ ) which are dissolved. In addition to these processes, long isotopic exchange between groundwater and the carbonated aquifer (carbonates dissolution–precipitation) in closed system condition is also contributing to further  $\delta^{13}\text{C}_{\text{DIC}}$  enrichment [31,36]. Isotopic compositions of soil CO<sub>2</sub> depend on the type of vegetation, in the range of  $\delta^{13}\text{C}_{\text{g}} = -20\text{‰}$  to  $-26\text{‰}$  VPDB (Vienna Pee Dee Belemnite) for C3 vegetation, and between  $-10\text{‰}$  and  $-15\text{‰}$  VPDB for C4 vegetation [20,36,37]. Studies carried out in the St. Lawrence Lowlands recall the endemic presence of C3 vegetation as woodlands and prairies [1], but enriched composition due to corn cultivation (C4 vegetation) is also possible and reported [38]. Isotopic composition of marine carbonate is typically of about  $\delta^{13}\text{C}_{\text{s}} \approx 0\text{‰}$  VPDB considering typical Ordovician carbonate compositions [39], which may vary within a narrow range of few permil [33].

Other source of salinity in the context of St. Lawrence–Lowlands may be associated with sulphate (SO<sub>4</sub><sup>2−</sup>) inputs like those from gypsum, releasing Ca<sup>2+</sup> and SO<sub>4</sub><sup>2−</sup> into groundwater. A reported source of Na<sup>+</sup> in the region is due to Ca–Na and Mg–Na cation exchanges [1], where Ca<sup>2+</sup> and Mg<sup>2+</sup> are preferentially adsorbed onto the clays, inducing the desorption and the release of Na<sup>+</sup> into groundwater [20]. Intensity of cation exchange may be evaluated by comparing the Na/Cl ratio in groundwater to the one expected from seawater origin (Na/Cl  $\approx$  0.86 [40]). In the case of the geomorphological context of Quebec, inputs of Na<sup>+</sup> and Cl<sup>−</sup> are usually inferred from the Champlain Sea marine invasion, as confined brackish water and/or pore water in low–permeability matrices and aquitards [34], and from long–term diffusion of Na–Cl from marine clay freshening [10].

### 3. Methods

#### 3.1. Passive Sampler Description and Design

Passive samplers were developed for the collection of non–gaseous solutes (e.g., major ions,  $\delta^2\text{H}$ ,  $\delta^{18}\text{O}$  and  $\delta^{13}\text{C}$  data presented in this work). The sampling is called “passive” as the equilibration at the inside of the sampler is reached through physically–driven

solute transport, without any action from mechanical or electrical devices. The principle of passive sampling is to place samplers in the wellbore until their content equilibrate with composition of the groundwater at the depth they are placed at. As the dominant physical process (e.g., molecular diffusion or convection) responsible for the equilibration is unknown, different equilibration tests were performed in controlled conditions in the laboratory. Laboratory testing is also essential to understand the kinetic of the equilibration and to ensure that samplers are left in wells long enough to accurately collect groundwater at depth with a pristine chemical composition.

The samplers consist of 0.5 L Nalgene high-density polyethylene bottles with a 2.5 cm diameter open Tygon tubing at the top (Figure 2). Prior to in situ positioning, the samplers are pre-filled with distilled and degassed water to minimize unwanted contribution of any solute from the outside of the well. Passive samplers are installed and centered at a chosen depth by fixing them to a weighted line trolled down into the wellbore. As soon as collected out of the wellbore, the water inside the upper tubing of the sampler is discarded to prevent collecting water mixtures that may occur when the sampler is trolled up to the surface. Once recovered, the samplers are immediately sealed without head space and their content is later dispatched into different vials at the laboratory for subsequent analysis. Transfers into vials using syringes are carefully operated to minimize contact with the atmosphere.

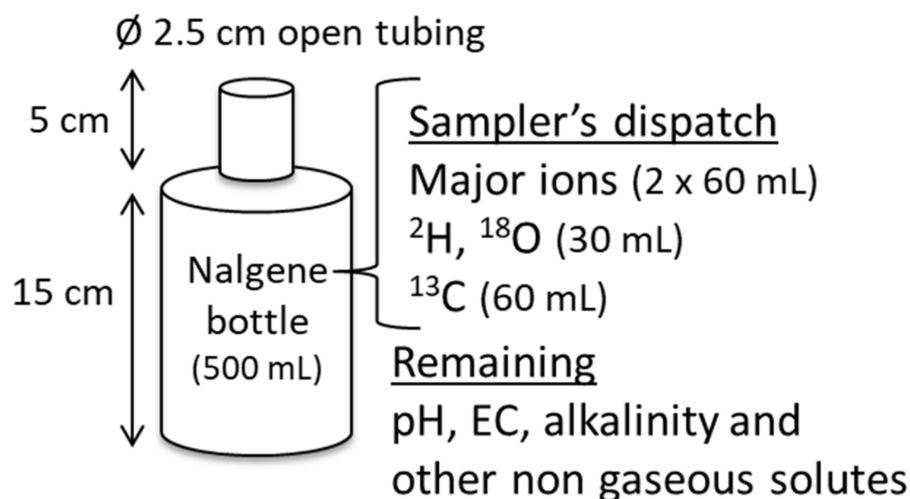


**Figure 2.** Groundwater passive sampler and dispatch to subsequent vials for analysis.

### 3.2. Passive Sampler Laboratory Testing

Equilibration tests were carried out in the laboratory with passive samplers (0.5 L) placed in water tanks (25 L) filled with different Na-Cl solutions (Figure 3). The electrical conductivity of the solutions was monitored during re-equilibration. The first test intended to reproduce the in situ manipulation, the sampler being filled with distilled water and having an initial temperature warmer than that of the environment (Figure 3a). The second test is carried under isothermal conditions for both containers, the sampler being filled with higher mineralized water (Figure 3b). The later test is designed to study the transport by molecular diffusion from the sampler to the tank.

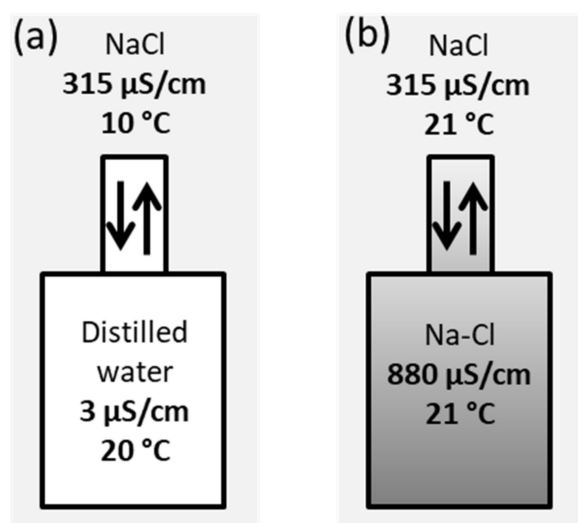


**Figure 3.** Laboratory re-equilibration tests for passive liquid samplers (a) sampler filled with distilled water, as used in situ, (b) sampler containing a solution more saline but similar temperature than its environment to only study molecular diffusion.

### 3.3. Passive Samplers' Placement Determined from Previous Physical Borehole Surveys

In the context of heterogeneous aquifers (implicitly including fractured aquifers), sequential passive sampling would benefit by being preceded by physical borehole investigations [23,41]. This allows addressing the distribution of the productive zones (Equation (1)), as well as to identify the occurrence of ambient flows, if any. Indeed, the recharge and discharge of aquifers commonly involve a minor vertical component that results in a vertical hydraulic head gradient. The latter is expressed by vertical ambient flows occurring into the boreholes [22,41]. Passive sampler placement is determined by the position of water inflows into the wellbore, downstream of each of them according to the flow direction in the water column (Figure 4). When the sampler is located outside of a mixing zone, the sampler directly collects the water composition associated with the fracture (i.e.,  $C_{z-1} = C_z^f$ , Figure 4). When the sampler is located within a mixing zone, the composition collected represents the mixing of upstream productive zones. Within mixing zones, the water composition relative to each fracture ( $C_z^f$ ) can be calculated by deconvoluting the compositions collected at adjacent samplers (Equation (2)).

$$Q_T = \sum_{z_{min}}^{z_{max}} q_z \quad (1)$$

$$C_z^f = \frac{(q_z + q_{z-1})C_z - q_{z-1}C_{z-1}}{q_z} \quad (2)$$

The physical parameters of the productive zones were measured out by borehole logging, using spinner flowmeter and optical surveys, with a particular focus on high-resolution temperature sensing. The summary of hydraulic characteristics (total well depth, casing length, depth to the water table, flow distribution), obtained from the pumping of all wellbores is shown in Figures 5 and 6. Details about these physical borehole surveys are described in previous published works [41,42]. The detection thresholds evaluated for the measurement of vertical water flows in wells with a diameter of 150 mm are, respectively, 1 L/min with the spinner flowmeter and 0.01 L/min with high-resolution temperature sensing [41].

Among the ten wells that were accessible for this study, the logging survey without pumping revealed the occurrence of flows already occurring permanently in six wells (i.e., those represented in Figure 5). Given the high flow rates measured, Napierville PO2, St. Roch, Mirabel and Ormstown wells are certainly influenced by nearby municipal pumping, inducing strong and forced bypass drainage through interconnected fractures.

For Napierville P6 and Hemmingford wells, flows in static conditions were not identified from spinner flowmeter surveying, but were highlighted by more sensitive temperature surveys, suggesting the occurrence of low and ambient flows.

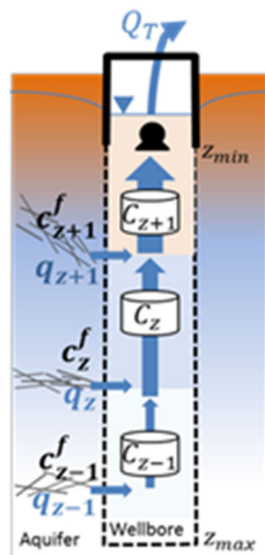


Figure 4. Representation of flow conditions and sampler placement in long screened wellbores during pumping.

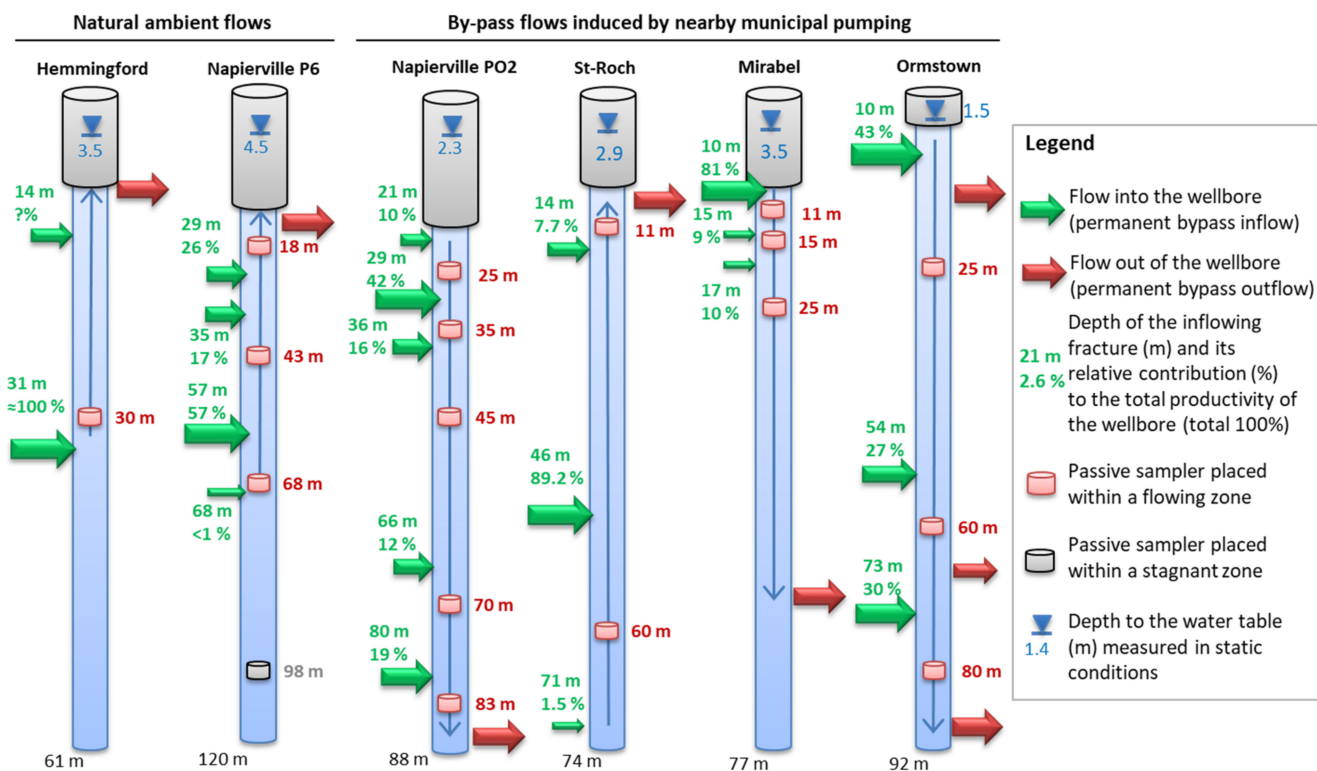
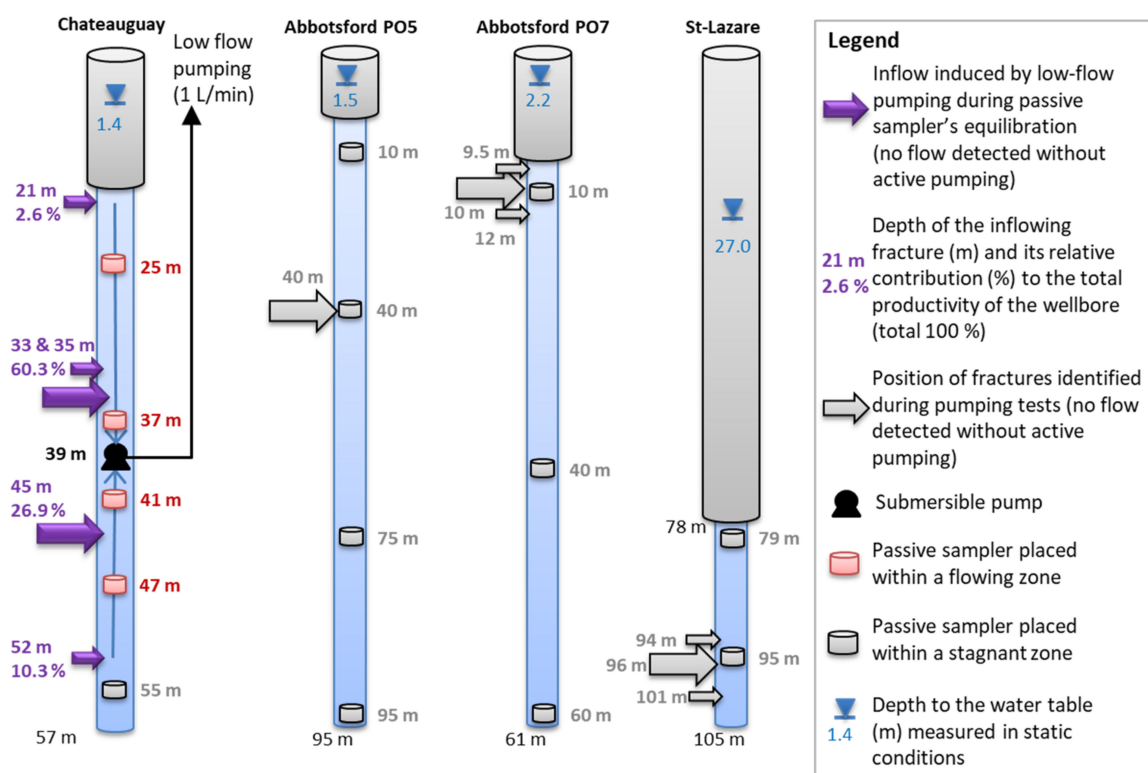


Figure 5. Placement of passive samplers for wells impacted by permanent flows (natural ambient flows and bypass flows induced by nearby municipal pumping).



**Figure 6.** Placement of passive samplers for wells having stagnant water column in static condition. Flows for Chateauguay were imposed by a permanent low flow pumping at a depth of 39 m in order to constrain water flows during passive sampler's equilibration.

For the other wellbores accessible for this study (i.e., Chateauguay, St. Lazare, Abbotsford PO5 and PO7, Figure 6), no detectable flows were reported by high-resolution temperature surveys in “static condition” (i.e., surveys performed without actively pumping the wellbore). The latter wellbores likely have stagnant water columns in static condition, and thus appeared not influenced by natural ambient flows or impacted by nearby municipal pumping. The flowing situation shown for Chateauguay in Figure 6 was latter induced by a low flow pumping at 39 m depth that was put in place to constrain water fluxes during samplers' equilibration.

The Chateauguay well has the most interesting investigation potential over all the chosen wells as it is not influenced by nearby pumping nor natural ambient flows, and has fractures relatively well distributed with depth. Chateauguay well was therefore more intensively sampled for geochemistry. A low flow pumping of 1 L/min, imposed at a depth of 39 m (Figure 6), was used to constrain the water fluxes during the 6-days period of passive sampling. This equilibration was set to much longer duration than the duration required for water passive samplers because other passive samplers for gases were simultaneously tested (data not presented here). Permanent low-flow pumping was ensured by a stand-alone station including a submersible pump powered by a solar panel. This set-up allowed the calculation of water composition at each fracture by deconvolution from those collected by the passive samplers (Equation (2)). Considering the high bypass flow observed in wells influenced by municipal pumping (i.e., those presented at Figure 5), it was not possible to constrain them with the stand-alone pumping system. Temperature surveys were immediately taken following the passive sampler collection and reported identical flow direction as when passive samplers were initially put in place. It was also impossible to ensure that such existing flow would remain constant over time during sampling so that the geochemistry for fractures located within mixing zones were not deconvoluted. The representativeness of depths indicated for geochemistry in all figures and tables (deconvoluted, within or outside of mixing zones) is detailed at the bottom of Table 1.

Table 1. Hydrogeochemical data gathered from passive sampling.

Lithology	Localization	Wellbore	Depth * (m)	T (°C)	pH	TDS mg/L	Water Type	Ca <sup>2+</sup> mg/L	Mg <sup>2+</sup> mg/L	Na <sup>+</sup> mg/L	K <sup>+</sup> mg/L	Alk. as HCO <sub>3</sub> <sup>-</sup> mg/L	Cl <sup>-</sup> mg/L	SO <sub>4</sub> <sup>2-</sup> mg/L	Na/Cl (molar)	δ <sup>2</sup> H ‰VSMOW	δ <sup>18</sup> O ‰VSMOW	δ <sup>13</sup> C ‰VPDB
Red schist	Abbotsford	PO5	10	8.5	8.2	531	Na,Mg— Cl,HCO <sub>3</sub>	27	29	110	3.1	181	150	31	1.1	-78.18	-11.31	
			40	8.4	8.3	515	Na,Mg— Cl,HCO <sub>3</sub>	26	30	120	0.3	157	150	32	1.2	-78.16	-11.32	
			75	8.4	8.1	1589	Na,Mg—Cl	120	120	330	0.6	99	910	9	0.6	-84.85	-11.98	
			95	8.5	8.2	1854	Na,Mg—Cl	150	140	370	0.6	87	1100	6	0.5	-86.00	-12.12	
		PO7	10	9.0	7.9	502	Ca— HCO <sub>3</sub> ,Cl	95	11	43	1.5	254	69	29	1.0	-77.14	-11.16	
			40	8.8	7.8	545	Ca,Na— HCO <sub>3</sub> ,Cl	95	14	58	1.3	254	89	34	1.0	-77.18	-11.22	
			60	8.7	7.8	720	Na,Ca— Cl,HCO <sub>3</sub>	64	17	160	1.2	266	170	42	1.5	-77.37	-11.22	
Sandstone	Hemmingford	P-Cl	30	9.0	7.2	370	Ca,Mg— HCO <sub>3</sub>	37	20	28	3.2	242	8.9	31	4.9	-79.72	-11.49	
	St. Lazare	P11	79	8.3	7.9	236	Ca,Mg— HCO <sub>3</sub>	32	11	8.2	2.2	181	0.6	0.5	21.1	-81.79	-11.95	-5.9
			95	8.4	7.7	237	Ca,Mg— HCO <sub>3</sub>	32	12	8.9	2.3	181	0.6	0.5	23.3	-81.80	-12.07	-6.6
	Ormstown	Dumas 10	10	8.2	7.5	553	Ca— SO <sub>4</sub> ,HCO <sub>3</sub>	100	21	16	4.9	187	14	210	1.8	-82.83	-12.12	-12.9
			60	8.2	7.5	580	Ca— SO <sub>4</sub> ,HCO <sub>3</sub>	110	19	15	4.7	199	12	220	1.9	-83.49	-11.71	
			80	8.2	7.4	610	Ca— SO <sub>4</sub> ,HCO <sub>3</sub>	120	20	15	4.6	168	13	270	1.8	-83.14	-12.23	
	Dolomite	Napierville	P6	18	8.3	7.4	2378	Ca,Mg—SO <sub>4</sub>	360	120	200	8.5	193	96	1400	3.2	-72.43	-10.21
43				8.2	7.2	2523	Ca,Mg—SO <sub>4</sub>	390	120	200	8.3	205	99	1500	3.1	-72.81	-10.38	-7.3
68				8.2	7.2	2556	Ca,Mg—SO <sub>4</sub>	380	130	210	8.3	217	110	1500	2.9	-73.01	-10.50	-7.3
98				8.2	7.1	2554	Ca,Mg—SO <sub>4</sub>	390	130	210	8.6	205	110	1500	2.9	-73.23	-10.21	
PO2			21	9.1	7.0	921	Ca— HCO <sub>3</sub> ,SO <sub>4</sub>	160	37	30	4.8	395	64	230	0.7	-72.05	-10.67	
			45	8.7	7.2	1179	Ca,Mg— SO <sub>4</sub> ,HCO <sub>3</sub>	190	47	43	5.1	291	43	560	1.5	-72.25	-10.64	
			70	8.6	7.2	1183	Ca— SO <sub>4</sub> ,HCO <sub>3</sub>	210	47	47	5.3	317	47	510	1.5	-72.54	-10.50	
83	8.6	7.2	1239	Ca,Mg— SO <sub>4</sub> ,HCO <sub>3</sub>	200	50	49	5.4	301	44	590	1.7	-71.89	-10.70				

Table 1. Cont.

Lithology	Localization	Wellbore	Depth * (m)	T (°C)	pH	TDS mg/L	Water Type	Ca <sup>2+</sup> mg/L	Mg <sup>2+</sup> mg/L	Na <sup>+</sup> mg/L	K <sup>+</sup> mg/L	Alk. as HCO <sub>3</sub> <sup>-</sup> mg/L	Cl <sup>-</sup> mg/L	SO <sub>4</sub> <sup>2-</sup> mg/L	Na/Cl (molar)	δ <sup>2</sup> H ‰VSMOW	δ <sup>18</sup> O ‰VSMOW	δ <sup>13</sup> C ‰VPDB
			21	8.3	7.9	460	Mg,Ca,Na— HCO <sub>3</sub>	43	29	37	5.1	339	8.9	6	6.4	-73.92	-10.72	-13.7
			<u>33–35</u>	8.2	7.7	532	Ca,Mg,Na— HCO <sub>3</sub>	51	30	53	5.1	304	44	55	1.9	-74.96	-10.89	-13.4
	Chateauguay	MELCC 03090013	<u>45</u>	8.1	7.7	546	Ca,Mg,Na— HCO <sub>3</sub>	52	29	51	4.9	305	44	57	1.7	-74.92	-10.85	-13.3
			52	8.1	7.7	566	Ca,Mg,Na— HCO <sub>3</sub>	55	32	55	5.5	314	50	63	1.7	-74.74	-11.02	-13.3
			55	8.0	7.5	575	Ca,Mg,Na— HCO <sub>3</sub>	54	32	59	5.5	304	67	60	1.4	-75.06	-10.93	-13.1
	Mirabel	Charles	10	9.9	6.9	849	Ca,Mg— HCO <sub>3</sub> ,SO <sub>4</sub>	110	43	57	4.1	355	100	180	0.9	-61.09	-8.99	-14.1
Limestone	St. Roch	2017–04	<b>11</b>	9.8	6.9	879	Ca,Mg— Cl,HCO <sub>3</sub>	120	59	41	8.1	353	230	68	0.3	-70.19	-10.53	-11.9
			71	9.2	7.2	919	Ca,Mg— Cl,HCO <sub>3</sub>	110	60	85	9.1	297	290	68	0.5	-71.45	-10.31	
Detection threshold/analytical error (±)								0.3	0.1	0.1	0.1	1	0.05	5.0	–	±1.5	±0.05	±0.1

\* **Bold**: depth of a sampler placed within a zone of water mixing; Underlined: depth of the inflowing fracture (deconvoluted concentration); **Grey**: depth of the sampler in stagnant water column; Normal: depth of the inflowing fracture out of a zone of water mixing. Nitrates were analyzed for all the samples but were not detected (detection threshold of 0.02 mg/L N–NO<sub>3</sub>).

### 3.4. Low Flow Sampling at Depth

For the Chateauguay well, duplicates of groundwater samples were taken by micro-pumping at the passive samplers' depths in order to cross validate both sampling methods. The sampling line consisted of 5 mm diameter high density polyethylene (HDPE) tubing and the pumping was ensured from a peristaltic pump operated from the surface. Prior to sampling, the tubing was rinsed with distilled water. Sampling was performed at low flow rates (0.5 L/min), with flushing duration long enough to ensure that at least five times the volume of the tubing was flushed out before sampling.

### 3.5. General Sampling and Analytical Procedures

Conductivity and pH were measured for each groundwater sample following the collection of passive samplers at the field. Samples for major ions were dispatched in 60 mL high-density polyethylene bottles. Samples for cations were filtered on site using disposable 0.45  $\mu\text{m}$  nitrocellulose filters and preserved with nitric acid. After filtration, samples for nitrates were preserved with sulphuric acid, using dedicated vials. All samples were kept at 4 °C until their analysis. Major ions ( $\text{Ca}^{2+}$ ,  $\text{Mg}^{2+}$ ,  $\text{Na}^+$ ,  $\text{K}^+$ ,  $\text{Cl}^-$ ,  $\text{SO}_4^{2-}$ ,  $\text{NO}_3^-$ ) were analyzed at the Maxxam Laboratory in Montreal (Quebec, Canada). Alkalinity was measured by Gran titration [43] at the University of Quebec in Montreal (UQAM) water geochemistry laboratory, by the day of the collection of the sample. Samples for stable isotopes of water and  $\delta^{13}\text{C}$  were, respectively, collected in 30 mL high-density polyethylene and 60 mL brown glass bottles without head space.

## 4. Results

### 4.1. Passive Sampler Testing in Laboratory

Results of the tests on the equilibration time required for collecting major ions in passive samplers are reported in Figure 7. When the sampler is filled with distilled water warmer and less mineralized than its environment, likely inducing natural convection (detailed below), equilibration is achieved within 4 h (Figure 7a). When only transport by molecular diffusion is occurring, equilibration is achieved after about 20 days (Figure 7b).

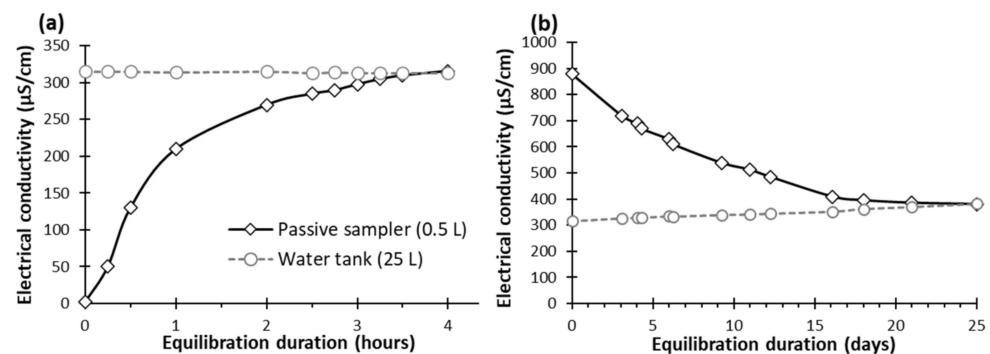


**Figure 7.** Equilibration results in laboratory: (a) conditions as implemented in situ (samplers filled with warmer distilled water), (b) equilibration soliciting only molecular diffusion (isothermal experience with higher mineralization into the sampler).

Measured equilibration time by soliciting only molecular diffusion (Figure 7b) is comparable to a theoretical diffusive transport of NaCl in a static water column (Figure 8). This latter is calculated considering  $D^*_{\text{NaCl}} = 7.9 \times 10^{-9} \text{ m}^2/\text{s}$  at 20 °C [44], using the analytical solution of Ogata–Banks [45] and considering only molecular diffusion (advection terms neglected). The latter calculation evaluates the transport by pure molecular diffusion in an open environment, neglecting wall effects inside the sampler that must lead to even slower solute transport.

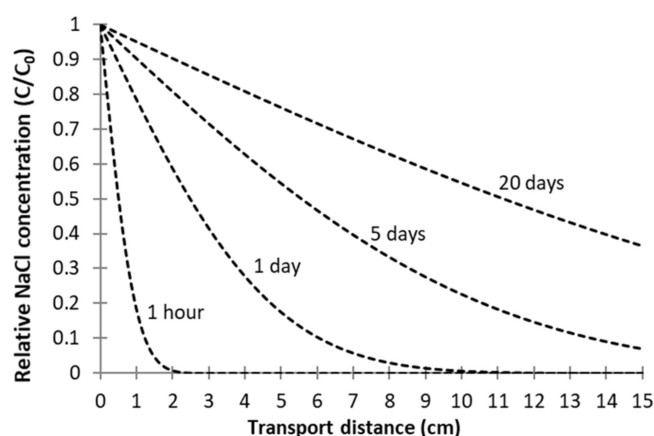


**Figure 8.** Theoretical breakthrough curves for the transport of NaCl by molecular diffusion in stagnant water at 20 °C.

Fast equilibration of the samplers within hours (Figure 7a) suggests that transport by molecular diffusion cannot be dominant. Indeed, theoretical transport evaluated for pure molecular diffusion (Figure 8) over a distance comparable to the height of the sampler (i.e., 15 cm) would be significant only at least after 20 days. The latter theoretical duration is comparable with results obtained when only molecular diffusion is solicited in laboratory tests (Figure 7b). Fast equilibration observed for the sampler as used for the in situ protocol (Figure 7a) must be driven by natural convection flux [46], initiated from slight differences of fluid density due to differences in temperature and/or solute concentration. Upwards convection currents are inferred from the inside of the sampler (warmer and less mineralized water) towards the water tank and would be simultaneously compensated by downwards convection currents from the water tank (colder and more mineralized water). These convection fluxes ultimately result in the rapid homogenization of the sampler with its environment. Such convective transport would always be solicited for in situ conditions as the samplers were pre-filled with warmer distilled water ( $T \geq 15$  °C as fieldwork was always performed during summer and fall), compared to groundwater which is necessarily more mineralized and colder all year long (i.e., from between 8 to 10 °C, and total dissolved solids (TDS) ranging from between 236 and 2556 mg/L, Table 1).

#### 4.2. Validation of Passive Sampling at Depth and Deconvolution at Fractures

The validation of passive sampling efficiency at depth was tested according to experiments performed at the Chateauguay wellbore. Samplers' concentrations collected after 6 days of equilibration are compared with samples collected by low flow pumping at the same depths (Table 2 and Figure 9).

**Table 2.** Concentrations measured at depths by passive sampling and by low flow pumping at the Chateauguay wellbore.

Sampling Mode	Depth (m)	pH	EC $\mu\text{S/cm}$	$\text{Ca}^{2+}$ mg/L	$\text{Mg}^{2+}$ mg/L	$\text{Na}^+$ mg/L	$\text{K}^+$ mg/L	$\text{HCO}_3^-$ mg/L	$\text{Cl}^-$ mg/L	$\text{SO}_4^{2-}$ mg/L	$\delta^{18}\text{O}$ ‰ VSMOW	$\delta^2\text{H}$ ‰ VSMOW
Passive Sampler	25	7.89	507	43	29	37	5	339	8.7	6.4	−10.71	−73.89
	37	7.7	667	51	30	52	5.1	305	43	53	−10.85	−74.62
	41	7.69	679	53	30	52	5	308	46	59	−10.88	−74.83
Low flow pumping	25	7.91	534	43	28	36	4.9	344	9.7	7.1	−10.75	−73.95
	37	7.81	621	47	27	48	4.9	300	38	39	−10.90	−75.07
	41	7.67	680	53	31	54	5.3	307	46	58	−10.91	−74.89
Detection threshold/ $\pm$ error %		0.1	5	0.3	0.1	0.1	0.1	1	0.05	0.5	$\pm 0.05$ ‰	$\pm 1.5$ ‰

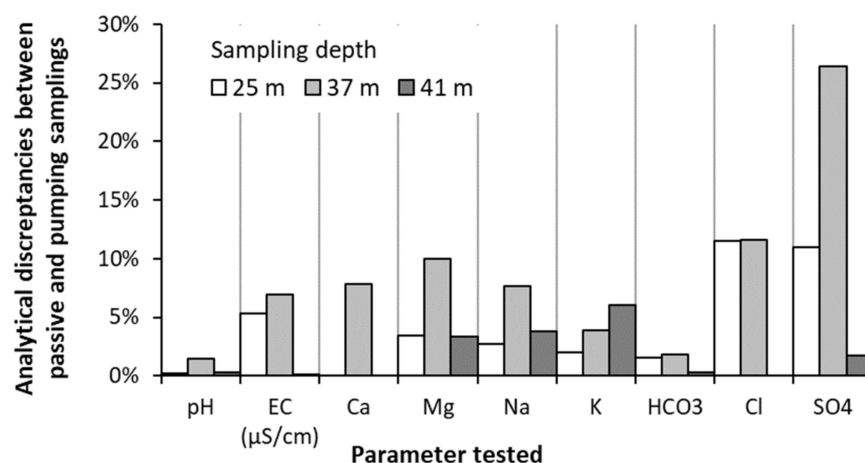


**Figure 9.** Analytical discrepancies between samples collected by passive samplers and those collected by low-flow pumping at different depths for the Chateauguy wellbore.

Electroneutrality errors for the samples (Table 2) were all below 3.9%. Of the 33 comparative measurements (11 parameters tested at three depths), the mean error is 2%. Four measurements of  $\text{Cl}^-$  and  $\text{SO}_4^{2-}$  at 25 and 37 m depths exceeded 10% of discrepancy (Figure 9). The largest discrepancy ( $\text{SO}_4^{2-}$ , 37 m) could be due to analytical errors or  $\text{SO}_4^{2-}$  reduction in the sample prior to analysis. Stable isotopes of water show good agreement between both sampling methods, with low discrepancies for  $\delta^{18}\text{O}$  and  $\delta^2\text{H}$  compositions, below the range of their analytical error. It is to be noted that low-flow sampling at depth appears to be more difficult to carry out than passive sampling, so that it can be a source of errors. Although the flow rate for sampling was deliberately limited to 0.25 L/min, the observed disparities may be induced by a change in the flow distribution in the water column during sampling (the permanent flow rate imposed being only 1 L/min). Additionally, even if the purging was carried out for a volume five times that of the tubing before sampling (i.e., 1 L to 1.6 L for HDPE tubing of 25 m to 41 m long, 0.3 cm diameter), it remains possible that the flushing of the tubing was not perfectly attained and affects the samples collected.

Another test was conducted at the Chateauguy wellbore to compare the chemical composition of the equivalent mixture calculated from the intensity and the composition (deconvoluted) at each fracture (from passive sampling), with the composition of the sample collected at the discharge of the main pumping. The comparison between physical parameters, major ions and stable isotopes are in good agreement, with differences of less than 5%, except for the electrical conductivity (10%) and  $\text{SO}_4^{2-}$  (14%) (Table 3).

**Table 3.** Comparison of passive sampling with samples collected at the pumping discharge of the Chateauguy wellbore.

	Depth (m)	pH	EC µS/cm	Ca <sup>2+</sup> mg/L	Mg <sup>2+</sup> mg/L	Na <sup>+</sup> mg/L	K <sup>+</sup> mg/L	HCO <sub>3</sub> <sup>-</sup> mg/L	Cl <sup>-</sup> mg/L	SO <sub>4</sub> <sup>2-</sup> mg/L	δ <sup>18</sup> O‰ VSMOW	δ <sup>2</sup> H‰ VSMOW
Passive Sampler	25	7.89	507	43	29	37	5	339	8.7	6.4	-10.71	-73.89
	37	7.7	667	51	30	52	5.1	305	43	53	-10.85	-74.62
	41	7.69	679	53	30	52	5	308	46	59	-10.88	-74.83
	47	7.72	715	55	32	55	5.3	314	50	63	-11.02	-74.74
Mixing (calculated from samplers)	7.70	672	52	30	52	5.1	308	44	54	-10.89	-74.74	
Pumping's discharge (sampled)	7.65	612	50	29	51	4.9	307	42	48	-10.89	-74.95	
% error	-1%	-10%	-4%	-4%	-2%	-4%	0%	-4%	-14%	0.004‰	0.21‰	
Detection threshold/±analytical error	±0.1	±5	0.3	0.1	0.1	0.1	1	0.05	0.5	±0.05‰	±1.5‰	

### 4.3. Hydrogeochemistry Gathered from Passive Sampling into the Wellbores

#### 4.3.1. Major Ions Composition

Twenty-nine (29) analyses for major ions are available for the 10 wells sampled (Table 1). All the water samples analyzed showed an electro-neutrality of less than 10%. Sample depths ranged from 10 to 98 m (mean 50 m). Water temperatures ranged from 8.0 to 9.9 °C (mean 8.5 °C), pH values from 6.9 to 8.3 (mean 7.5) and total dissolved solids (TDS) from 236 to 2 556 mg/L (mean 975). Water types are predominantly Ca–HCO<sub>3</sub> (40%), Ca–SO<sub>4</sub> (37%), Na–Cl (17%) and Ca–Cl (7%). Although Mg<sup>2+</sup> never appears as the major cation (exception for Chateauguay 21 m), it represents at least a quarter of the cationic mineralization in 70% of the samples. Geochemical data table is provided in Table 1. Nitrates were analyzed in all groundwater samples, but all the results reported concentrations below the detection limit of 0.02 mg/L N–NO<sub>3</sub>. The results below essentially focus on the weathering of carbonates, as most of the wellbores are installed in carbonate aquifers, and because unconsolidated glacial sediments overlying the bedrock are widespread and their matrix contains carbonates.

Total dissolved solids (TDS) appear generally lower for the shallowest samples in each wellbore, but then do not vary at greater depths (Figure 10). On the other hand, TDS vary greatly from one well to another. Most elevated salinity is clearly associated with Ca–SO<sub>4</sub> water type (Napierville P6 and PO2, Table 1), as well as Cl<sup>−</sup> rich water type (deep samples of Abbotsford PO5). The size of the symbols for each sample in Figure 10 is relative to the depth, and this symbology is also used in Figures 12 to 14.

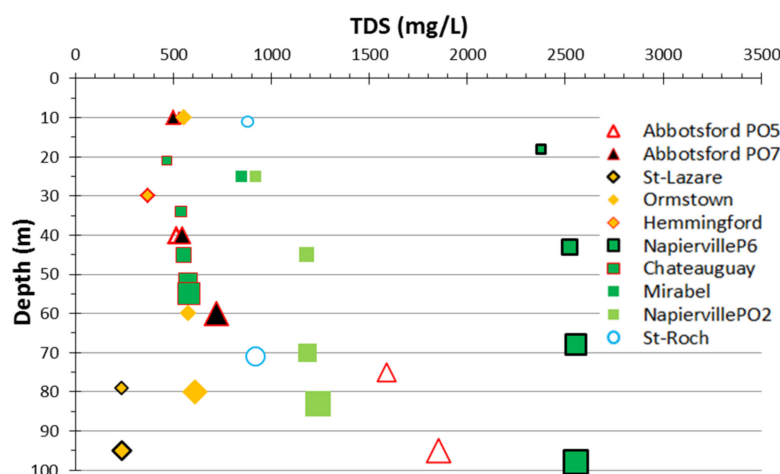


**Figure 10.** TDS as a function of depth and lithology (red—schist, orange—sandstone, green—dolomite and blue—limestone).

The ionic composition of the sample is illustrated with a Stabler Diagram (Figure 11) which allows comparing the relative proportion of anions and cations together. All samples analyzed have an electroneutrality error below 10%. At first sight (Figure 11), total alkalinity is the main source of salinity for 41% of the samples (St. Lazare, Hemmingford, Chateauguay, Mirabel and the shallowest sample of Abbotsford PO7) and relates to the calc–carbonic system. Then, salinity is primarily associated with SO<sub>4</sub><sup>2−</sup> rich waters for 34% of the samples (Ormstown and Napierville PO2 and P6). Finally, 24% of the sample’s mineralization is associated with chloride’s salt inputs (St. Roch, Abbotsford PO5 and deepest samples of Abbotsford PO7). By comparing anionic and cationic distribution (Figure 11), it appears that cationic composition cannot be always and simply explained by the three main hydrogeochemical processes usually described for the St. Lawrence Lowlands (i.e., carbonates dissolution, saline input from the Champlain sea invasion and inputs from gypsum). For example, SO<sub>4</sub><sup>2−</sup> concentrations for Napierville P6 do not balance with Ca<sup>2+</sup> and largely exceed it, suggesting other sources of salinity than just inputs from Ca–SO<sub>4</sub>. For Abbotsford PO5 indeed, Cl<sup>−</sup> concentrations do not balance with Na<sup>+</sup>, also

suggesting several inputs of chloride's salts than just from Na–Cl. Detail about the origin of these salinities is discussed in Section 5.

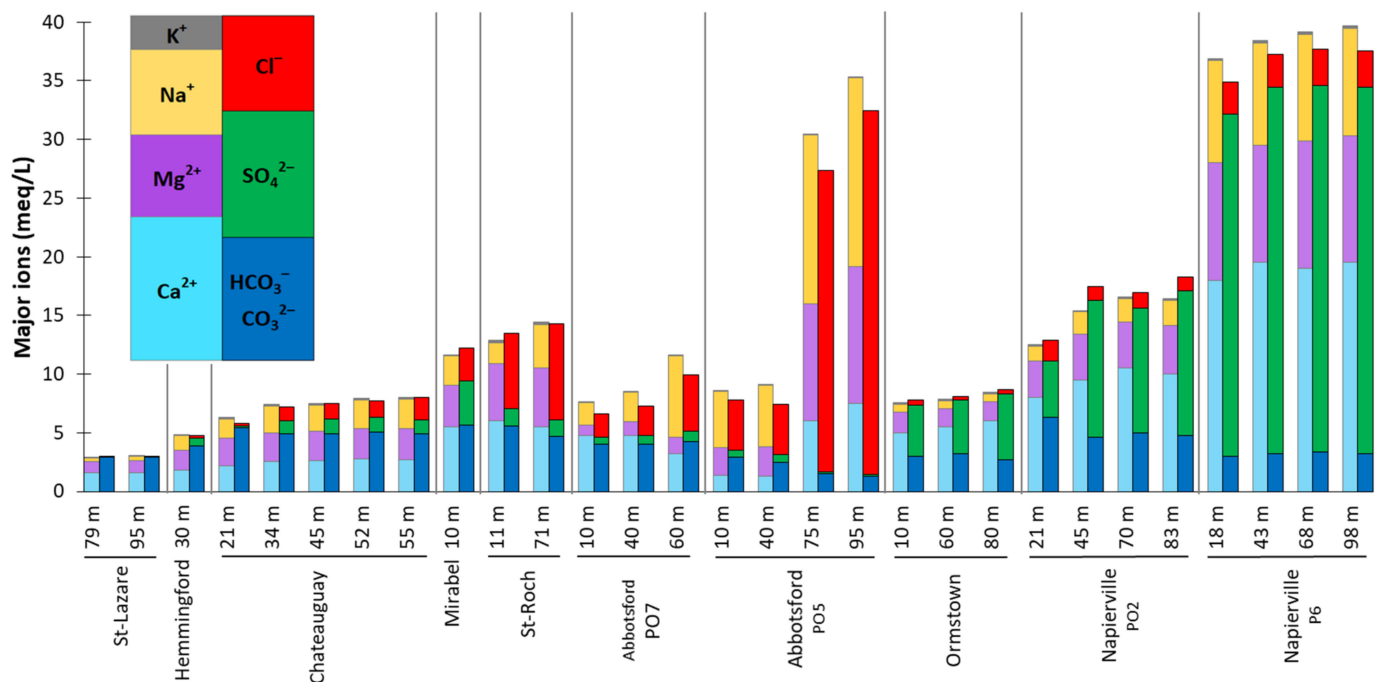


Figure 11. Stabler diagram detailing the major ion composition per wellbore and at depths.

To prepare the discussion about the origin of the ionic composition observed (Section 5), potential inputs of Ca<sup>2+</sup> and Mg<sup>2+</sup> from chloride salts are evaluated by subtracting other sources (from sulphate minerals and from carbonate dissolution) as given at Equation (3). Na<sup>+</sup> inputs from chloride salts are evaluated by subtracting calculated inputs of Ca<sup>2+</sup> and Mg<sup>2+</sup>, to the total amount of Cl<sup>-</sup> (Equation (4)). This mass balance is neglecting K<sup>+</sup> as it is of minor contribution in samples presented for this study (Figure 11, Table 1).

$$(\text{Ca} + \text{Mg})_{\text{chloride salts}} = (\text{Ca} + \text{Mg})_{\text{sample}} - \text{Alkalinity} - \text{SO}_4^{2-} \text{ (meq/L)} \quad (3)$$

$$\text{Na}_{\text{chloride salts}} = \text{Cl}^- - (\text{Ca} + \text{Mg})_{\text{chloride salts}} \text{ (meq/L)} \quad (4)$$

Illustration of the mass balance for the chloride salts is given in Figure 12 for samples composition largely dominated by Cl<sup>-</sup> inputs. For St. Roch wellbore, 40% of Ca<sup>2+</sup> and Mg<sup>2+</sup> would originate from chloride salts (Y-axis in Figure 12). For the two deepest samples of Abbotsford PO7, about 20% of Ca<sup>2+</sup> and Mg<sup>2+</sup> would originate from chloride salts, while the shallowest sample does not show any of such Ca<sup>2+</sup> and Mg<sup>2+</sup> inputs. For Abbotsford PO5, Ca<sup>2+</sup> and Mg<sup>2+</sup> contributions from chloride salts are relatively weak for the two shallowest samples (between 5 and 15%), while they account for about 90% of the salinity for the two deepest samples.

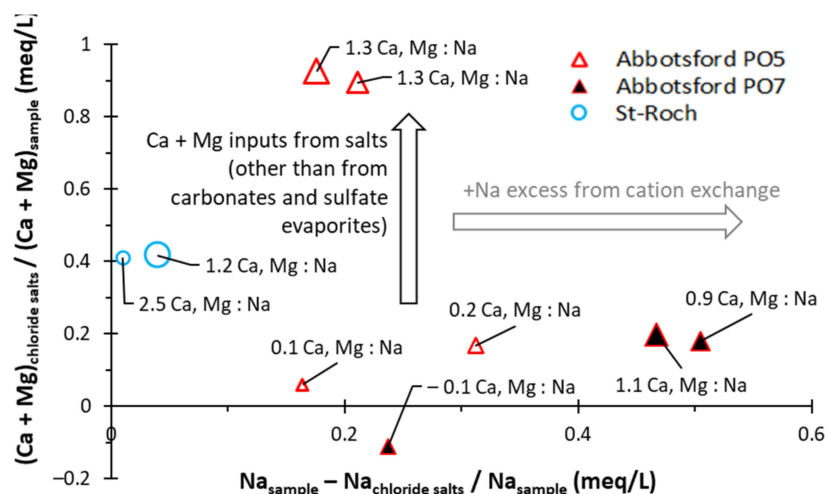


**Figure 12.** Ratio of Ca<sup>2+</sup>, Mg<sup>2+</sup> and Na<sup>+</sup> contributions from chloride salts evaluated in the samples showing an anionic composition dominated by Cl<sup>-</sup> (St. Roch and Abbotsford wellbores).

#### 4.3.2. Calco–Carbonic System and δ<sup>13</sup>C

Partial CO<sub>2</sub> pressure for each sample was computed using PHREEQC and are presented in Figure 13 as a function of pH, alkalinity, as well as the typical pCO<sub>2</sub> at the recharge (i.e., soils and atmosphere). Saturation equilibrium curves towards calcite were also computed with PHREEQC (mean temperature of groundwater: 8.5 °C), considering theoretical fully open and closed systems with different pCO<sub>2</sub> ranges (i.e., modelling of equilibrium at calcite saturation, with a solution under constant pCO<sub>2</sub>, or with a solution having initial but not replenished pCO<sub>2</sub>). Arrows depicts the evolution in theoretical open and closed systems as well as for “partially open system” (introduced in Section 3.2) that conceptually correspond to open condition prevailing at the recharge and within the unsaturated zone, followed by and evolution in closed condition within the saturated zone.

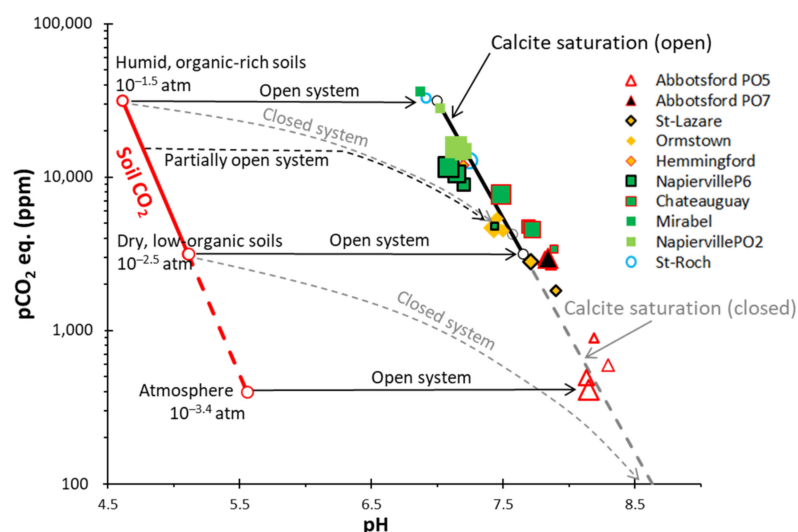


**Figure 13.** (Modified from Clark [32]): Samples pCO<sub>2</sub> as a function of pH, shown together with saturation equilibriums for calcite and pCO<sub>2</sub> at the recharge (soil and atmosphere).

The isotopic composition of dissolved inorganic carbon (δ<sup>13</sup>C<sub>DIC</sub>) in the sampled groundwater can be visualized in Figure 14, along with δ<sup>13</sup>C<sub>g</sub> from C3 and C4 vegetation, and with δ<sup>13</sup>C<sub>DIC</sub> endmembers at calcite saturation. The DIC and pH end members for open and closed systems conditions are calculated with PHREEQC. Considering a fully open system (theoretical), δ<sup>13</sup>C<sub>DIC</sub> endmembers on Figure 14 correspond to the enrichment

due to the fractionation ( $\epsilon_{\text{CO}_2/\text{DIC}}$ ) between soil  $\text{CO}_2$  and the DIC. This fractionation is calculated using the weighted enrichment contributions of each DIC species ( $\text{H}_2\text{CO}_3$ ,  $\text{HCO}_3^-$ ,  $\text{CO}_3^{2-}$ ) at given pH [33] and at 8.5 °C (mean temperature of the groundwater samples, Table 1). Considering a fully closed system (theoretical),  $\delta^{13}\text{C}_{\text{DIC}}$  endmembers are calculated considering that half of the carbon from soil  $\text{CO}_2$  ( $\delta^{13}\text{C}_g$ ) is diluted (and enriched) with carbon ( $\delta^{13}\text{C}_s$ ) from carbonates weathering (calcite and dolomite weathering at Equations (5) and (6)).

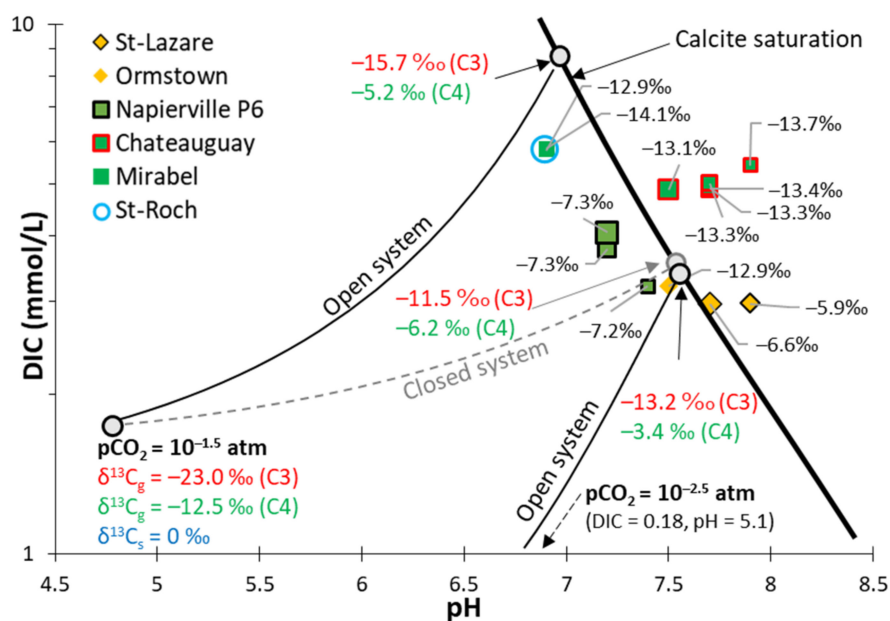
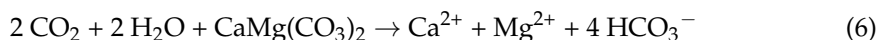
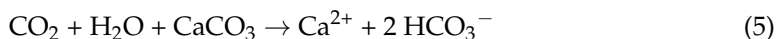


**Figure 14.** (Modified from Clark & Fritz [33]):  $\delta^{13}\text{C}_{\text{DIC}}$ , DIC and pH of the samples represented with  $\delta^{13}\text{C}$  endmembers, for open and closed system conditions towards soil  $\text{CO}_2$ , C3 and C4 vegetation  $\delta^{13}\text{C}_g$  and different soil  $\text{pCO}_2$ . For an open system,  $\delta^{13}\text{C}_{\text{DIC}}$  fractionation ( $\epsilon_{\text{CO}_2/\text{DIC}}$ ) at calcite saturation is considered between soil  $\text{CO}_2$  and weighted contribution of each DIC species, and calculated at 8.5 °C. For closed system, a dilution of  $\delta^{13}\text{C}_g$  by half of  $\delta^{13}\text{C}_s$  from carbonates is considered.

#### 4.3.3. Stable Isotopes of Water

Stable isotope of water ( $\delta^2\text{H}$ ,  $\delta^{18}\text{O}$ ) compositions collected by passive sampling at depth are reported in Figure 15a, as well as precipitation data collected in a station close to the St. Lazare area [47]. Isotopic compositions follow the local meteoric water line, indicating that the waters infiltrated contributing to the recharge did not undergo any significant surface evaporation compared to the precipitations, as otherwise  $\delta^2\text{H}$  and  $\delta^{18}\text{O}$  enrichments would be observed [32].  $\delta^2\text{H}$  and  $\delta^{18}\text{O}$  compositions at each well appear not to vary with the depth (Except for two deepest samples of Abbotsford PO5, Figure 15b), but vary from one site to another, i.e., heavier isotope composition being observed for Mirabel, and a lighter composition for Abbotsford and St. Lazare wellbores.

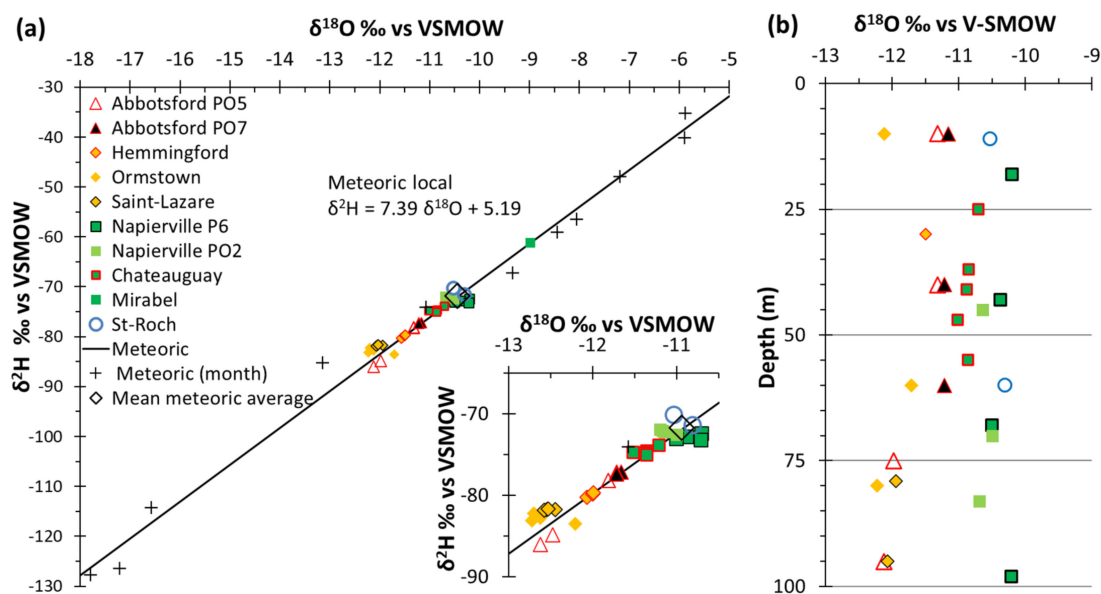


Figure 15. (a)  $\delta^{18}\text{O}$  and  $\delta^2\text{H}$  compositions in groundwater and in local precipitation. (b)  $\delta^{18}\text{O}$  composition with the depth.

## 5. Discussions

### 5.1. Representativeness of the Sequential Sampling with Depth in Fractured Aquifers

All the wells investigated showed a heterogeneous distribution of fractures that are discrete and rather isolated (Figures 5 and 6). A frequent occurrence of multidirectional bypass flows within the wellbores is observed (Figure 5). Sampling these aquifers must therefore be preceded by borehole logging. Without such preliminary physical survey, criteria such as “sampling depth” or “total well depth” might become obsolete for any interpretation regarding the chemical stratification of groundwater. When the composition of water at each inflowing fracture is to be determined, flows into the well must be constrained during passive sampling (i.e., Chateauguay well example). The placement of the pump constraining the flows at intermediate depth into the wellbore is relevant for optimizing the resolution of the sequential sampling. Following the example of the Chateauguay well (Figure 6), the sampler placed at 25 m depth collects the composition of the fracture at 21 m, and the one at 47 m collects the composition of the fracture at 52 m. The compositions of samplers placed at the 37 and 41 m represent mixed water inflows, but only from two consecutive fractures.

In fractured aquifers, the quality of passive sampling is optimal when water flows are present in the water column, as the composition of the sampler represents the composition of the water column at the sampled depth. If the water column is stagnant, the composition of the sampler after equilibration is theoretically that of the mixture between the stagnant water in the vicinity of the sampler and the initial content of the sampler. It is difficult however to imagine a perfectly stagnant water column in a fractured aquifer or in each long-screened wellbore, because of the natural convection [46] induced by density difference (temperature and/or solute concentrations), or because of the widespread occurrence of very low but permanent ambient flows [22,23]. However, if we consider the mixture between the distilled water within the sampler (0.5 L) with the stagnant groundwater corresponding to one meter of water column (i.e., 17 L for a 150 mm diameter borehole), the dissolved species collected in the sampler would be impacted by a bias of 3% with respect to groundwater composition. Considering the high bypass flow rates observed in wells influenced by municipal pumping (Figure 5), it was not possible to constrain them with the stand-alone pumping system. As it was also impossible to ensure that such existing flows would remain constant over time during sampling, the concentration at fractures were not deconvoluted.

## 5.2. Sources of Groundwater Salinity and Respective Contributions

### 5.2.1. Calco–Carbonic Systems

When alkalinity dominates anionic mineralization (for St. Lazare, Hemmingford, Chateauguay, Mirabel and at the shallowest sample of Abbotsford PO7 wellbores, Figure 11),  $\text{Ca}^{2+}$  and  $\text{Mg}^{2+}$  originating from the dissolution of carbonates (calcite and dolomite, Equations (5) and (6)) balance accurately with the alkalinity. This mineralization from carbonate weathering is comparable with the data gathered from regional studies conducted in the St. Lawrence Lowlands, which reports TDS ranging from 150 to 500 mg/L [11,14,47,48]. System openness to soil  $\text{CO}_2$  is discussed hereafter as it determines the amount of carbonates that can be ultimately weathered by the groundwater (Section 3.2). Given that depths to the water table are shallow for all sites but St. Lazare (i.e., from 1.4 to 4.5 m, Figures 5 and 6), residence times through the unsaturated zones are likely short. At the contrary, St. Lazare unsaturated zone consists of a 27 m thick sandy deposit that would imply more significant openness to soil  $\text{CO}_2$  before reaching the saturated zone. Except for Abbotsford PO5, all  $\text{pCO}_2$  are in the range expected from an evolution from soil  $\text{pCO}_2$  ( $\gg$  atmospheric  $\text{pCO}_2$ , Figure 14). System openness to soil  $\text{CO}_2$  for St. Roch and Mirabel appears greater compared to the other wellbores.  $\text{pCO}_2$  for these two sites are near or above the maximum expected for soils (i.e.,  $10^{-1.5}$  for humid organic-rich soils, Figure 13), have rather acidic pH and highest elevated DIC (Figure 13). The latter suggesting for these two sites great openness towards soil  $\text{CO}_2$ , even acquired within thin unsaturated zones (depths to the water table  $<3.5$  m, Figure 5), likely followed by limited and short evolution in closed system conditions within the saturated zone as calcite saturation is not even reached (Figures 13 and 14). System openness for Abbotsford PO5 appears the weakest of all samples since it has the lowest  $\text{pCO}_2$ , suggesting that groundwater for Abbotsford PO5 has more strongly evolved in closed system condition (within the saturated zone), and/or that  $\text{pCO}_2$  inherited from the recharge conditions may have been much lower compared to other sites. The  $\text{pCO}_2$  (Figure 13), alkalinity,  $\text{Ca}^{2+}$  and  $\text{Mg}^{2+}$  concentrations (Figure 11) as well as the saturation towards calcite (Figures 13 and 14) resulting from carbonate weathering vary little with the depth but are different from one well to another, thus depending on each site-specific openness to soil  $\text{CO}_2$ . Since no difference is observed at depth for each wellbore, the calco–carbonic mineralization would be reached rapidly by water percolating within the unsaturated zone and/or within the first few meters of the saturated zone, as also reported by [31,49].

### 5.2.2. Mineralization from $\text{SO}_4^{2-}$ Inputs

When  $\text{SO}_4^{2-}$  dominates the anionic composition, high concentrations for  $\text{Ca}^{2+}$  and  $\text{Mg}^{2+}$  are likely associated with slow dissolution of carbonates still containing residual evaporite salts, or presence of brackish waters derived from evaporite dissolution in low-permeable and stagnant zones of the aquifer. Given work previously published in the region that reported low concentration of  $\text{SO}_4^{2-}$  in deep brines [50], diffusion of  $\text{SO}_4^{2-}$  from deep-seated sedimentary units is unlikely. Sulphate-rich evaporites may consist of gypsum ( $\text{Ca-SO}_4$ ) and epsomite ( $\text{Mg-SO}_4$ ) [51], respectively, responsible for  $\text{Ca}^{2+}$  and  $\text{Mg}^{2+}$  occurrence in groundwater. The highest  $\text{SO}_4^{2-}$  concentrations are found in Napierville P6 well, where they represent more than 80% of the anionic salinity, two third of them being attributed to  $\text{Ca-SO}_4$  and one third to  $\text{Mg-SO}_4$  (Figure 11). Napierville waters are reaching TDS of 1500 to 2000 mg/L due to  $\text{SO}_4^{2-}$  inputs.  $\text{Ca-SO}_4$  waters were reported in the regional studies within the St. Lawrence Lowlands, being sparsely present for some sites but not exceeding TDS of 500 mg/L [11,14], or reporting similar TDS as high as of 1000 to 1800 mg/L for few samples in dolomitic aquifers [47]. The origin of  $\text{SO}_4^{2-}$  in the Napierville groundwater would be natural, as no anthropogenic sources of  $\text{SO}_4^{2-}$  were identified in the area.

### 5.2.3. Mineralization from $\text{Cl}^-$ Inputs

The other main source of salinity is associated with Ca,Mg,Na-Cl, referred hereafter as “chloride salts”. Regional studies [11,14] reported the presence of brackish waters, with salinity exceeding 500 mg/L and reaching as much as 2500 mg/L and sourced by the Champlain sea invasion. Groundwater collected in this work having dominant  $\text{Cl}^-$  inputs exceeding 500 mg/L, with a maximum of 1800 mg/L are found in the Abbotsford PO5 well at 95 m depth. When  $\text{Cl}^-$  is the dominant anion, molar Na/Cl ratios are as low as 0.28 and 0.52 for St. Roch–71 m and Napierville P6–95 m, respectively, implying that seawater inputs (Na/Cl  $\approx$  0.86) is not always the main source of  $\text{Cl}^-$  and/or that other processes are source of  $\text{Na}^+$  (see below), provoking Na/Cl disbalancing. Sources of Ca,Mg-rich chloride salts may be related to the formation of evaporites, with associated brines, and/or by the pollution from road de-icing salts. Ca, Mg, Na: Cl’s brine formed during the formation of evaporites may percolates and accumulates at greater depths in the sedimentary column [52]. An example of Ca, Mg rich brine (average meq/L ratio of 1.8 Ca, Mg:Na) was found in the study area of St. Laurence Lowlands and are described by [50], reaching TDS of about 100 to 300 g/L in Cambrian and Ordovician sedimentary formations and at depths of about 800 to 1400 m. De-icing road salt may also be the source  $\text{Na}^+$  as well as  $\text{Ca}^{2+}$  and  $\text{Mg}^{2+}$  chloride salts.  $\text{MgCl}_2$  and  $\text{CaCl}_2$  are reported to be regularly added to de-icing salt mixtures in Quebec, as for reaching lower eutectic temperature (i.e., respectively,  $-33\text{ }^\circ\text{C}$  and  $-55\text{ }^\circ\text{C}$ ), compared to  $-21\text{ }^\circ\text{C}$  with the use of Na-Cl alone [53]. Given the composition of the samples for St. Roch and Abbotsford wellbores, inputs from road salt or from fossil brines are both possible. However,  $\delta^2\text{H}$  and  $\delta^{18}\text{O}$  isotopic composition of these waters follow the meteoric water line (Figure 15) while fossil brines show often anomalous  $\delta^2\text{H}$  compositions above the meteoric line [54]. Furthermore, fossil brines are found at depths of several hundred meters [50]. Based on these considerations, we suggest that rich inputs of  $\text{Ca}^{2+}$  and  $\text{Mg}^{2+}$  from chloride salts for St. Roch and Abbotsford wellbores are more likely due to de-icing road salt pollution. The latter sites being, respectively, placed within an urban area, and in a rural area but at less than 300 m from main roads. Highest salinities observed at greater depths for Abbotsford PO5 (75 and 95 m) are inferred to be the result of the density driven accumulation of road salt’s pollution at the bottom of the wellbore, where stagnant water condition is maintained due to the extremely low permeability of the fractured aquifer at this location, whereas all the other wellbores are located in much productive aquifers.

### 5.2.4. Other Mineralization Related to $\text{Na}^+$ Inputs

For samples dominated by  $\text{Cl}^-$  inputs (St. Roch and Abbotsford), excess of  $\text{Na}^+$  compared to that expected from chloride salts (X-axis of Figure 12), is likely attributed to Ca-Na and Mg-Na cation exchange occurring in the aquifer. Na input from cation exchange appear insignificant for St. Roch samples, while it is reaching from 18% to 50% in Abbotsford samples. For wellbore not dominated by chloride salts inputs, Na/Cl ratios are in the vast majority greater than the one expected from seawater (Na/Cl  $\approx$  0.86), which is an evidence that cation exchange is widespread for Hemmingford, St. Lazare, Ormstown, Napierville, Chateauguay and Mirabel wellbores (Table 1). Part of  $\text{Na}^+$  or  $\text{Ca}^{2+}$  contributions from Ca and Na-Feldspar weathering cannot be completely excluded, especially for wells installed in the sandstone aquifer (St. Lazare, Ormstown). However, as carbonates are present within Quaternary sediments overlaying the fractured aquifer, and present even in few amounts in the cement of the sandstone [55], significant contributions of Ca from silicate weathering over carbonates weathering is very unlikely. Regarding Na excess, Ca-Na cation exchange is reported in the region to be effective even for quite evolved groundwater [1,12,13], suggesting that the ion exchange capacity is still available after relatively long residence time of groundwater within the aquifer. Significant Na inputs from plagioclase weathering appears unlikely in the context of this study for all wellbores but St. Lazare for which it is possible. Silicate weathering is indeed much more resilient

that carbonate weathering [33], and groundwater at all sites (but St. Lazare) appears to be “recent” (Section 5.3).

### 5.3. Complementary Information Gathered from Isotopic Geochemistry

All the groundwater samples have isotopic composition ( $\delta^{18}\text{O}$  and  $\delta^2\text{H}$ ) that are depleted compared to the yearly average of precipitations (Figure 15a). This would be the result of more intense recharge periods during spring snow melt and fall rainfall as suggested by recharge studies in Quebec [56], whose isotopic composition being depleted compared to other precipitations periods in the study area [47]. Different isotopic compositions are observed from one well to another, but do not show depth-dependent variability within each well (Figure 15b). Different isotopic compositions are thus attributable to site specific distribution of seasonal intensity of the recharge. Discriminating between remnants of Champlain seawater or depleted Pleistocene melt water that may have accumulated at great depths is not possible using stable isotopes of water. Champlain seawater composition (i.e.,  $\delta^{18}\text{O} \approx -10.5\text{‰}$  as reported by [34]) would be in the same range as the mean meteoric composition of the study area (i.e.,  $\delta^{18}\text{O} \approx -10.5\text{‰}$ , Figure 15a) and  $\delta^{18}\text{O}$  isotopic shift between today and the last glacial period is only of 1.5‰ VSMOW (Vienna Standard Mean Ocean Water) [57] and falls within the observed isotopic variability in wells studied.

Data presented for  $\delta^{13}\text{C}$  in Figure 14 are complementing the discussion about the evolution of water regarding the calco-carbonic system and its openness to soil  $\text{CO}_2$  (Section 5.2.1), and to infer about potential contemporary sources of carbon at the recharge. The first notice is that except for St. Lazare (where no sample is available at shallow depths), the samples do show no variation of the  $\delta^{13}\text{C}_{\text{DIC}}$  with the depth. The second notice is that except for St. Lazare and Napierville P6, all the samples have a  $\delta^{13}\text{C}_{\text{DIC}}$  of about  $-13\text{‰}$ . Such isotopic composition would correspond to “recent” groundwater that evolved from C3  $\delta^{13}\text{C}_g$  contributions at the recharge (i.e.,  $\delta^{13}\text{C}_g \approx -23\text{‰}$  for endemic vegetation of Quebec) and reach calcite saturation with corresponding dilution and enrichment from carbonates ( $\delta^{13}\text{C}_s \approx 0\text{‰}$ ). Long and significative interaction with carbonated aquifer is unlikely as it would lead to greater  $\delta^{13}\text{C}_{\text{DIC}}$  enrichment, at least above  $-11.5\text{‰}$  (i.e.,  $\delta^{13}\text{C}_{\text{DIC}} = -11.5\text{‰}$  is reached at calcite saturation for closed system condition from  $\delta^{13}\text{C}_g \approx -23\text{‰}$ , half diluted with  $\delta^{13}\text{C}_s \approx 0\text{‰}$ ). For all samples but St. Lazare and Napierville P6, the two notices presented above suggest the presence of well mixed and “recent” groundwater bodies at all depths, that likely did not undergo long interaction with the carbonated aquifer. For Napierville P6,  $\delta^{13}\text{C}_{\text{DIC}}$  composition of  $-7.2\text{‰}$  VPDB can be explained by potential contribution of  $\delta^{13}\text{C}_g$  from C4 vegetation ( $\delta^{13}\text{C}_g \approx -12.5\text{‰}$ ) as corn fields are present around this site, as well as possible presence of “old” water bodies that undergo long interaction with the carbonated aquifer. However, the presence of old water bodies for Napierville P6 at all depths appears inconsistent with unconfined conditions inferred at this site (Section 2.1), and because saturation towards calcite is not even reached for all these samples (Figures 13 and 14). Thus, it is believed that groundwater at Napierville P6 are “recent”, impacted by contemporary C4 vegetation (corn fields) and well mixed overall within the aquifer. The case of St. Lazare is more complicated as  $\delta^{13}\text{C}_{\text{DIC}}$  are as enriched as  $-5.9$  and  $-6.6\text{‰}$  VPDB, but no data is available at shallow depths to argue about potential  $\delta^{13}\text{C}_{\text{DIC}}$  enrichment ( $\epsilon_{\text{CO}_2/\text{DIC}}$  fractionation) within the vadose zone and/or due to long water/carbonate aquifer interaction within the saturated zone at depth. St. Lazare site has a thick unsaturated zone (27 m) that would likely lead to  $\delta^{13}\text{C}_{\text{DIC}}$  enrichment because of fractionation with soil  $\text{CO}_2$  before reaching the saturated zone. St. Lazare wellbore is installed in sandstone (Potsdam Group) composed of up to 99% of quartzite with a clayey cementation [27]. However, it is also reported that the cement of this sandstone can contains calcite in variable proportion [55], so that  $\delta^{13}\text{C}_{\text{DIC}}$  evolution due to long interaction with carbonate within the Potsdam sandstone cannot be excluded. Heavy  $\delta^{13}\text{C}_{\text{DIC}}$  measured for St. Lazare can also very well be the result of significant contributions of C4 carbon from effluents of individual residential septic systems that are numerous in this area. Such impact from septic system remains however relatively unlikely as nitrates

were not detected within the St. Lazare Samples. However, given data available only at depth greater than 79 m, and without other insights from other tracers, it is unfortunately not possible to argue about the presence of recent or ancient groundwater, or a mix of both, within the St. Lazare aquifer.

#### 5.4. Flowing Systems Inferred from Hydrogeochemistry within the Fractured Aquifers

All the observations concerning mineralization from the calco-carbonic system,  $\text{SO}_4^{2-}$  and  $\text{Cl}^-$  inputs, road salt pollution and stable isotopes ( $\delta^{13}\text{C}$ ,  $\delta^2\text{H}$  and  $\delta^{18}\text{O}$ ) indicate for each site similar water bodies that do not vary greatly with the depth, suggesting the presence of strong mixing conditions in the fractured aquifers investigated.  $\text{SO}_4^{2-}$  contributions may slightly increase with the depth (Figures 10 and 11), still suggesting prevalent mixing conditions at all depths but the presence of some less permeable zones at depth. It is believed that higher salinities found at depths for the Abbotsford wellbores would be the result of accumulation of road salt's pollution in stagnant water at the bottom of the wellbore, due to extremely low permeability of the aquifer at depth at this location. Otherwise, mixing conditions appear to generally prevail in productive fractured aquifers down to depths of about 100 m (maximum depth investigated). The residence times of the water bodies cannot be quantified without the use of other environmental tracers, but the available data suggest significant contributions of contemporary water according to anthropogenic pollution (road salts, C4 carbon sources) typical of the post-industrial area (post 1950), and poorly evolved waters according to the  $\delta^{13}\text{C}$ . It is likely that quick flows are effective because of the low secondary porosity of the fractured aquifers (reported as low as 1% on average for the studied wellbores [42]), and that the mixing of water until great depths is possible because of an overall well interconnected distribution of fractures into the aquifer. Both of these effects apparently prevail in natural conditions (i.e., as for Chateauguay wellbore), but are very likely enhanced by nearby municipal pumping (as for the situation of more than half of the wellbores studied) which are modifying natural flowing regime by inducing forced drainage of the aquifers.

## 6. Conclusions

Through laboratory testing, the equilibration of passive samplers was demonstrated to be achieved within 4 h. The use of passive samplers appears particularly suitable and relatively simple for the sequential sampling of solutes regarding groundwater quality (major ions) and for stable isotopes ( $\delta^2\text{H}$ ,  $\delta^{18}\text{O}$  and  $\delta^{13}\text{C}$ ). Regardless of the method, the interpretation of the chemistry gathered through sequential sampling in fractured aquifers is strongly enhanced when coupled with borehole logging investigations within long screened wellbores. Otherwise, "sampling depth" and/or "total wellbore depth" become ambiguous parameters regarding the interpretation of the groundwater chemistry with the depth. The sequential sampling campaign is generally pointing at not significant hydrogeochemical stratification within the wellbores investigated. As inferred from ionic composition, pollution from de-icing road salts and stable isotopes, groundwater bodies appear relatively well mixed among "recent" groundwater contributions for depth up to 100 m, especially, but not only, when the wellbores are influenced by nearby anthropogenic withdrawal. Although the fractures observed in the wells are generally discrete and relatively few in number, the finding of mixed water observed up to significant depths suggests that the fracture networks are extensive and well interconnected overall. Such findings are also pointing to the fact that the water resource is available and likely vulnerable to contamination from the surface, even at significant depths in the fractured aquifer. Quantitative estimation of groundwater residence time is not presented in this present article, but further work implying the passive sampling of other environmental tracers would be highly valuable to improve and to specify the understanding of the flow systems in place.

Finally, since vertical hydrogeochemical stratification is not prevalent over a depth of 100 m, conventional sampling of the pumped mixture at the wells would have given

similar results as those currently presented with the use of sequential sampling. It is possible in these conditions that the use of sequential sampling in fractured aquifers of the study area is rather relevant at depths exceeding 100 m and for wells likely crosscutting different sedimentary permeable formations. However, there are no such data available to suggest at what depth the hydrogeochemical stratification would become significant in the region. Furthermore, given the very limited number of wells studied in this work, the weak hydrogeochemical stratification until depth of 100 m cannot be generalized because in certain places, and according to different contexts that have not yet been explored, such chemical stratification may be more apparent within 100 m of depth.

**Author Contributions:** Conceptualization, G.M. and F.B.; Data curation, G.M.; Funding acquisition, G.M., F.B., J.-M.L. and R.M.; Investigation, G.M.; Methodology, G.M., F.B. and J.C.A.; Resources, F.B., J.-M.L. and R.M.; Supervision, F.B. and J.C.A.; Validation, G.M., F.B., J.C.A. and D.L.P.; Writing—original draft, G.M., J.C.A. and D.L.P.; Writing—review and editing, G.M., F.B., J.C.A., D.L.P., J.-M.L. and R.M. All authors have read and agreed to the published version of the manuscript.

**Funding:** This research was funded by the Natural Sciences and Engineering Research Council of Canada, grant “For’Age—Outils de datation pour la protection de la ressource en eau souterraine exploitée au Canada” (RDCPJ 514535–17).

**Institutional Review Board Statement:** Not applicable.

**Informed Consent Statement:** Not applicable.

**Data Availability Statement:** Data sharing is not applicable to this article as all geochemical results are presented in Table 1. The data as spreadsheet are however available on request from the corresponding author.

**Acknowledgments:** The authors would like to thank the Quebec Ministry of Environment (*Ministère de l’Environnement et de la Lutte contre les Changements Climatiques*) who kindly provided access to some of the sampling locations, and to the Natural Sciences and Engineering Research Council of Canada from which this research was made possible through a collaborative grant in industrial partnership with hydrogeologists teams of TechnoRem and Envir’Eau-Puits. The latter providing most accesses to the study sites, support and expertise regarding the hydrogeological conditions of the areas investigated.

**Conflicts of Interest:** The authors declare no conflict of interest.

## References

1. Cloutier, V.; Lefebvre, R.; Savard, M.M.; Bourque, É.; Therrien, R. Hydrogeochemistry and groundwater origin of the Basses-Laurentides sedimentary rock aquifer system, St. Lawrence Lowlands, Québec, Canada. *Hydrogeol. J.* **2006**, *14*, 573–590. [[CrossRef](#)]
2. Mattei, A.; Barbecot, F.; Goblet, P.; Guillon, S. Pore water isotope fingerprints to understand the spatiotemporal groundwater recharge variability in ungauged watersheds. *Vadose Zone J.* **2020**, *19*, 20066. [[CrossRef](#)]
3. Edmunds, W.M.; Cook, J.M.; Darling, W.G.; Kinniburgh, D.G.; Miles, D.L.; Bath, A.H.; Morgan-Jones, M.; Andrews, J.N. Baseline geochemical conditions in the Chalk aquifer, Berkshire, U.K.: A basis for groundwater quality management. *Appl. Geochem.* **1987**, *2*, 251–274. [[CrossRef](#)]
4. Mendizabal, I.; Stuyfzand, P.J.; Wiersma, A.P. Hydrochemical system analysis of public supply well fields, to reveal water–quality patterns and define groundwater bodies: The Netherlands. *Hydrogeol. J.* **2011**, *19*, 83–100. [[CrossRef](#)]
5. Larocque, M.; Cloutier, V.; Levison, J.; Rosa, E. Results from the Quebec Groundwater Knowledge Acquisition Program. *Can. Water Resour. J. Rev. Can. Ressour. Hydr.* **2017**, *43*, 69–74. [[CrossRef](#)]
6. Blanchette, D.; Lefebvre, R.; Nastev, M.; Cloutier, V. Groundwater Quality, Geochemical Processes and Groundwater Evolution in the Chateauguay River Watershed, Quebec, Canada. *Can. Water Resour. J. Rev. Can. Res. Hydr.* **2010**, *35*, 503–526. [[CrossRef](#)]
7. Benoit, N.; Nastev, M.; Blanchette, D.; Molson, J. Hydrogeology and hydrogeochemistry of the Chaudière River watershed aquifers, Québec, Canada. *Can. Water Resour. J. Rev. Can. Res. Hydr.* **2014**, *39*, 32–48. [[CrossRef](#)]
8. Montcoudiol, N.; Molson, J.; Lemieux, J.M. Groundwater geochemistry of the Outaouais Region (Québec, Canada): A regional-scale study. *Hydrogeol. J.* **2014**, *23*, 377–396. [[CrossRef](#)]
9. Boucher, C.; Pinti, D.L.; Roy, M.; Castro, M.C.; Cloutier, V.; Blanchette, D.; Larocque, M.; Hall, C.M.; Wen, T.; Sano, Y. Groundwater age investigation of eskers in the Amos region, Quebec, Canada. *J. Hydrol.* **2015**, *524*, 1–14. [[CrossRef](#)]
10. Ghesquière, O.; Walter, J.; Chesnaux, R.; Rouleau, A. Scenarios of groundwater chemical evolution in a region of the Canadian Shield based on multivariate statistical analysis. *J. Hydrol. Reg. Stud.* **2015**, *4*, 246–266. [[CrossRef](#)]

11. Vautour, G.; Pinti, D.L.; Méjean, P.; Saby, M.; Meyzonnat, G.; Larocque, M.; Castro, M.C.; Hall, C.M.; Boucher, C.; Roulleau, E.; et al.  $3\text{H}/3\text{He}$ ,  $14\text{C}$  and  $(\text{U}-\text{Th})/\text{He}$  groundwater ages in the St. Lawrence Lowlands, Quebec, Eastern Canada. *Chem. Geol.* **2015**, *413*, 94–106. [[CrossRef](#)]
12. Saby, M.; Larocque, M.; Pinti, D.L.; Barbecot, F.; Sano, Y.; Castro, M.C. Linking groundwater quality to residence times and regional geology in the St. Lawrence Lowlands, southern Quebec, Canada. *Appl. Geochem.* **2016**, *65*, 1–13. [[CrossRef](#)]
13. Walter, J.; Chesnaux, R.; Cloutier, V.; Gaboury, D. The influence of water/rock—Water/clay interactions and mixing in the salinization processes of groundwater. *J. Hydrol. Reg. Stud.* **2017**, *13*, 168–188. [[CrossRef](#)]
14. Beaudry, C.; Lefebvre, R.; Rivard, C.; Cloutier, V. Conceptual model of regional groundwater flow based on hydrogeochemistry (Montréal Est, Québec, Canada). *Can. Water Res. J.* **2018**, *43*, 152–172. [[CrossRef](#)]
15. Chaillou, G.; Touchette, M.; Buffin-Bélanger, T.; Cloutier, C.-A.; Héту, B.; Roy, M.-A. Hydrogeochemical evolution and groundwater mineralization of shallow aquifers in the Bas-Saint-Laurent region, Québec, Canada. *Can. Water Res. J.* **2018**, *43*, 136–151. [[CrossRef](#)]
16. Bondu, R.; Cloutier, V.; Rosa, E.; Roy, M. An exploratory data analysis approach for assessing the sources and distribution of naturally occurring contaminants (F, Ba, Mn, As) in groundwater from southern Quebec (Canada). *Appl. Geochem.* **2020**, *114*, 104500. [[CrossRef](#)]
17. Vogel, J.C. *Investigation of Groundwater Flow with Radiocarbon Isotopes in Hydrology*; International Atomic Energy Agency: Vienna, Austria, 1967; pp. 355–369.
18. Corcho Alvarado, J.A.; Purtschert, R.; Barbecot, F.; Chabault, C.; Rueedi, J.; Schneider, V.; Aeschbach-Hertig, W.; Kipfer, R.; Loosli, H.H. Constraining the age distribution of highly mixed groundwater using  $39\text{Ar}$ : A multiple environmental tracer ( $3\text{H}/3\text{He}$ ,  $85\text{Kr}$ ,  $39\text{Ar}$ , and  $14\text{C}$ ) study in the semiconfined Fontainebleau Sands Aquifer (France). *Water Res. Res.* **2007**, *43*. [[CrossRef](#)]
19. Visser, A.; Broers, H.P.; Purtschert, R.; Sültenfuß, J.; De Jonge, M. Groundwater age distributions at a public drinking water supply well field derived from multiple age tracers ( $85\text{Kr}$ ,  $3\text{H}/3\text{He}$ , and  $39\text{Ar}$ ). *Water Resour. Res.* **2013**, *49*, 7778–7796. [[CrossRef](#)]
20. Appelo, C.A.J.; Postma, D. *Geochemistry, Groundwater and Pollution*, 2nd ed.; A.A. Balkema Publishers: Leiden, The Netherlands, 2005; p. 649.
21. Mayo, A.L. Ambient well-bore mixing, aquifer cross-contamination, pumping stress, and water quality from long-screened wells: What is sampled and what is not? *Hydrogeol. J.* **2010**, *18*, 823–837. [[CrossRef](#)]
22. Alvarado, J.A.C.; Barbecot, F.; Purtschert, R. Ambient vertical flow in long-screen wells: A case study in the Fontainebleau Sands Aquifer (France). *Hydrogeol. J.* **2009**, *17*, 425–431. [[CrossRef](#)]
23. Poulsen, D.L.; Cook, P.G.; Simmons, C.T.; Solomon, D.K.; Dogramaci, S. Depth-Resolved Groundwater Chemistry by Longitudinal Sampling of Ambient and Pumped Flows Within Long-Screened and Open Borehole Wells. *Water Res. Res.* **2019**, *55*, 9417–9435. [[CrossRef](#)]
24. Tiedeman, C.R.; Hsieh, P.A. Assessing an Open-Well Aquifer Test in Fractured Crystalline Rock. *Groundwater* **2001**, *39*, 68–78. [[CrossRef](#)]
25. Clark, T.H. Montreal Area. Department of Natural Resources, General Direction of Mines, Geological Exploration Service. Available online: <http://gq.mines.gouv.qc.ca/documents/EXAMINE/RG152/RG152.pdf> (accessed on 14 September 2020).
26. Tremblay, A.; Pinet, N. Distribution and characteristics of Taconic and Acadian deformation, southern Québec Appalachians. *GSA Bull.* **1994**, *106*, 1172–1181. [[CrossRef](#)]
27. Globensky, Y. *Géologie des Basses-Terres du Saint-Laurent*; Rapport MM85-02; Direction Générale de l'Exploitation Géologique et minérale: Québec, QC, Canada, 1987; p. 70.
28. Parent, M.; Occhietti, S. Late Wisconsinan Deglaciation and Champlain Sea Invasion in the St. Lawrence Valley, Québec. *Géogr. Phys. Quatern.* **1988**, *42*, 215–246. [[CrossRef](#)]
29. Lamothe, M. A New Framework for the Pleistocene Stratigraphy of the Central St. Lawrence Lowland, Southern Québec. *Géogr. Phys. Quatern.* **1989**, *43*, 119–129. [[CrossRef](#)]
30. Nadeau, S.; Rosa, E.; Cloutier, V. Stratigraphic sequence map for groundwater assessment and protection of unconsolidated aquifers: A case example in the Abitibi-Témiscamingue region, Québec, Canada. *Can. Water Resour. J. Rev. Can. Res. Hydriq.* **2017**, *43*, 113–135. [[CrossRef](#)]
31. Gillon, M.; Barbecot, F.; Gibert, E.; Alvarado, J.A.C.; Marlin, C.; Massault, M. Open to closed system transition traced through the TDIC isotopic signature at the aquifer recharge stage, implications for groundwater  $14\text{C}$  dating. *Geochim. Cosmochim. Acta* **2009**, *73*, 6488–6501. [[CrossRef](#)]
32. Clark, I.D. *Groundwater Geochemistry and Isotopes*; CRC Press: Boca Raton, FL, USA, 2015.
33. Clark, I.D.; Fritz, P. *Environmental Isotopes*; Hydrology Lewis Publishers: Boca Raton, FL, USA, 1997.
34. Cloutier, V.; Lefebvre, R.; Savard, M.M.; Therrien, R. Desalination of a sedimentary rock aquifer system invaded by Pleistocene Champlain Sea water and processes controlling groundwater geochemistry. *Environ. Earth Sci.* **2010**, *59*, 977–994. [[CrossRef](#)]
35. Barbecot, F.; Marlin, C.; Gibert, E.; Dever, L. Hydrochemical and isotopic characterisation of the Bathonian and Bajocian coastal aquifer of the Caen area (northern France). *Appl. Geochem.* **2000**, *15*, 791–805. [[CrossRef](#)]
36. Han, L.-F.; Plummer, L.N.; Aggarwal, P. A graphical method to evaluate predominant geochemical processes occurring in groundwater systems for radiocarbon dating. *Chem. Geol.* **2012**, *318–319*, 88–112. [[CrossRef](#)]
37. Fontes, J.-C.; Garnier, J.-M. Determination of the initial  $14\text{C}$  activity of the total dissolved carbon: A review of the existing models and a new approach. *Water Resour. Res.* **1979**, *15*, 399–413. [[CrossRef](#)]

38. Cane, G.; Clark, I.D. Tracing Ground Water Recharge in an Agricultural Watershed with Isotopes. *Groundwater* **1999**, *37*, 133–139. [[CrossRef](#)]
39. Keith, M.; Weber, J. Carbon and oxygen isotopic composition of selected limestones and fossils. *Geochim. Cosmochim. Acta* **1964**, *28*, 1787–1816. [[CrossRef](#)]
40. Dickson, A.G.; Goyet, C. *Handbook of Methods for the Analysis of the Various Parameters of the Carbon Dioxide System in Sea Water*; Version 2 ORNL/CDIAC-74; Oak Ridge National Lab.: Oak Ridge, TN, USA, 1994.
41. Meyzonnat, G.; Barbecot, F.; Corcho-Alvarado, J.A.; Tognelli, A.; Zeyen, H.; Mattei, A.; McCormack, R. High-Resolution Wellbore Temperature Logging Combined with a Borehole-Scale Heat Budget: Conceptual and Analytical Approaches to Characterize Hydraulically Active Fractures and Groundwater Origin. *Geofluids* **2018**, *2018*, 9461214. [[CrossRef](#)]
42. Meyzonnat, G.; Barbecot, F.; Alvarado, J.A.C.; Lauzon, J.-M.; McCormack, R.; Tognelli, A.; Zeyen, H.; Alazard, M. Borehole Heat Budget Calculator: A New Tool for the Quick Exploitation of High-Resolution Temperature Profiles by Hydrogeologists. *J. Water Resour. Prot.* **2019**, *11*, 122–147. [[CrossRef](#)]
43. Stumm, W.; Morgan, J.J. *Aquatic Chemistry: Chemical Equilibria and Rates in Natural Waters*, 3rd ed.; John Wiley & Sons, Inc.: New York, NY, USA, 1996; p. 1022.
44. Zogzas, N.; Maroulis, Z. Effective Moisture Diffusivity Estimation from Drying Data. A Comparison between Various Methods of Analysis. *Dry. Technol.* **1996**, *14*, 1543–1573. [[CrossRef](#)]
45. Ogata, A.; Banks, R.B. *A Solution of the Differential Equation of Longitudinal Dispersion in Porous Media: Fluid Movement in Earth Materials*; US Government Printing Office: Washington, DC, USA, 1961.
46. Spitler, J.D.; Javed, S.; Ramstad, R.K. Natural convection in groundwater-filled boreholes used as ground heat exchangers. *Appl. Energy* **2016**, *164*, 352–365. [[CrossRef](#)]
47. Larocque, M.; Meyzonnat, G.; Baretche, D.; Graveline, M.; Ouellet, M. *Projet de Connaissance des Eaux Souterraines de la Zone de Vaudreuil–Soulanges—Rapport Scientifique. Rapport Déposé au Ministère du Développement Durable, de l’Environnement et de la Lutte Contre les Changements Climatiques*; Université du Québec à Montréal: Montreal, QC, Canada, 2015; p. 202.
48. Carrier, M.-A.; Lefebvre, R.; Rivard, C.; Parent, M.; Ballard, J.-M.; Benoit, N.; Vigneault, H.; Beaudry, C.; Malet, X.; Lauren-celle, M.; et al. Portrait des ressources en eau souterraine en Montérégie Est, Québec, Canada. In *Projet Réalisé Conjointement par l’INRS, la CGC, l’OBV Yamaska et l’IRDA dans le Cadre du Programme d’Acquisition de Connaissances sur les Eaux Souterraines*; Rapport Final INRS R-1433; Institut National de la Recherche Scientifique: Québec, QC, Canada, 2013; p. 319.
49. Gillon, M.; Barbecot, F.; Gibert, E.; Plain, C.; Alvarado, J.A.C.; Massault, M. Controls on  $^{13}\text{C}$  and  $^{14}\text{C}$  variability in soil C2. *Geoderma* **2012**, *189–190*, 431–441. [[CrossRef](#)]
50. Pinti, D.L.; Béland-Otis, C.; Tremblay, A.; Castro, M.C.; Hall, C.M.; Marcil, J.S.; Lapointe, R. Fossil brines preserved in the St. Lawrence Lowlands, Québec, Canada as revealed by their chemistry and noble gas isotopes. *Geochim. Cosmochim. Acta* **2011**, *75*, 4228–4243. [[CrossRef](#)]
51. Garrett, D.E. *Handbook of Lithium and Natural Calcium Chloride*; Elsevier Academic Press: Cambridge, MA, USA, 2004.
52. Garrett, D.E. *Potash: Deposits, Processing, Properties and Uses*; Chapman & Hall: London, UK, 1996; p. 734.
53. Charbonneau, P. Sels de voirie: Une utilisation nécessaire mais lourde de conséquences. *Nat. Can.* **2006**, *130*, 75–81.
54. Warr, O.; Giunta, T.; Onstott, T.C.; Kieft, T.L.; Harris, R.L.; Nisson, D.M.; Lollar, B.S. The role of low-temperature  $^{18}\text{O}$  exchange in the isotopic evolution of deep subsurface fluids. *Chem. Geol.* **2021**, *561*, 120027. [[CrossRef](#)]
55. Grenier, J.-F. *Caractérisation Pétrographique et Pétrophysique du Groupe de Potsdam dans le Forage A203, Basses-Terres du Saint-Laurent*; Mémoire de Maîtrise INRS; Institut National de la Recherche Scientifique: Québec, QC, Canada, 2014; p. 162.
56. Barbecot, F.; Guillon, S.; Pili, E.; Larocque, M.; Gibert-Brunet, E.; Hélie, J.-F.; Noret, A.; Plain, C.; Schneider, V.; Mattei, A.; et al. Using Water Stable Isotopes in the Unsaturated Zone to Quantify Recharge in Two Contrasted Infiltration Regimes. *Vadose Zone J.* **2018**, *17*, 170170. [[CrossRef](#)]
57. Caley, T.; Roche, D.M.; Waelbroeck, C.; Michel, E. Oxygen stable isotopes during the Last Glacial Maximum climate: Perspectives from data-model (LOVECLIM) comparison. *Clim. Past* **2014**, *10*, 1939–1955. [[CrossRef](#)]